Mechanistic Investigation of Cycloreversion/ Cycloaddition Reactions between Zirconocene Metallacycle Complexes and Unsaturated Organic Substrates†

Rebecca L. Zuckerman and Robert G. Bergman*

Department of Chemistry and Center for New Directions in Organic Synthesis (CNDOS), University of California, Berkeley, California 94720-1460

Received February 7, 2001

Treatment of the diazametallacycle $Cp_2Zr(N(t\text{-}Bu)C{=}N(SiMe_3)N(SiMe_3))$ (**4a**) with diphenylacetylene resulted in the formation of the azametallacyclobutene $Cp_2Zr(N(t\text{-}Bu)C(Ph){=}C(Ph))$ (**6a**) and $Me_3SiN{=}C{=}NSiMe_3$ in high yield. A kinetic study using UV−vis spectroscopy was carried out on the transformation. Saturation kinetic behavior was observed for the system, which is supportive of a mechanism that involves a reversible formal [2 + 2] retrocycloaddition of **4a** to generate the transient imido species $Cp_2Zr{=}N\text{-}t\text{-}Bu$ (**7a**) and $Me_3SiN{=}C{=}NSiMe_3$. Trapping **7a** with diphenylacetylene in an overall [2 + 2] cycloaddition reaction affords zirconacycle **6a**. The study of cycloreversion/cycloaddition reactions between diazametallacycle complexes and diphenylacetylene was extended to other zirconocene systems. Detailed kinetic studies were performed for the exchange reactions between the diazametallacycle complexes $Cp_2Zr(N(2,6\text{-}Me_2Ph)C{=}N(SiMe_3)N(SiMe_3))$ (**8a**) and $Cp_2Zr(N(2,6\text{-}Me_2Ph)C{=}N(t\text{-}Bu)N(t\text{-}Bu))$ (**8b**) with diphenylacetylene (**5a**) to give the corresponding azametallacyclobutene complex $Cp_2Zr(N(2,6\text{-}Me_2Ph)C(Ph){=}C(Ph))$ (**6c**) and extruded carbodiimides ($Me_3SiN{=}C{=}NSiMe_3$ for **8a** and $(t\text{-}Bu)N{=}C{=}N(t\text{-}Bu)$ for **8b**). For both systems, the reactions were found to be first order in metallacycle and zero order in alkyne. Treatment of the diazametallacycle complexes $Cp_2Zr(N(2,6\text{-}i\text{-}Pr_2Ph)C{=}N(Cyc)N(Cyc))$ (**9a**) and $Cp_2Zr(N(2,6\text{-}i\text{-}Pr_2Ph)C{=}N(i\text{-}Pr_2)N(i\text{-}Pr_2))$ (**9b**) with alkyne **5a** resulted in the formation of the six-membered zirconacycles **10a**,**b**, respectively, upon heating at 75 °C. The products **10a**,**b** are generated from the overall insertion of alkyne **5a** into the nitrogen−carbon bond of the zirconium-containing diazacyclobutane. Complex **10a** has been characterized by an X-ray crystallographic study. When the azacyclobutene $Cp_2Zr(N(2,6\text{-}i\text{-}Pr_2Ph)C(Ph){=}C(Ph))$ (**6e**) was treated with $CycN{=}C{=}NCyc$ or $(i\text{-}Pr)N{=}C{=}N(i\text{-}Pr)$, the same six-membered zirconacycle complexes **10a**,**b** were obtained. Kinetic analysis of the reaction of **6e** and $(i\text{-}Pr)N{=}C{=}N(i\text{-}Pr)$ to yield **10b** supports an associative process wherein alkyne **5a** directly inserts into the zirconium−carbon bond of **6e**. The diazametallacycle complex **4a** underwent a stoichiometric metathetical exchange with symmetrical carbodiimides $RN{=}C{=}NR$ (R = *p*-Tol, *m*-Tol, *i*-Pr, Cyc) to generate new cyclic zirconocene complexes and $Me_3SiN{=}C{=}NSiMe_3$. Kinetic studies were carried out on the exchange reaction between **4a** and $(m\text{-}Tol)N{=}C{=}N(m\text{-}Tol)$ to form **4e** and $Me_3SiN{=}C{=}NSiMe_3$. The experimental rate data obtained are consistent with a dissociative mechanism. Additionally, the saturation rate constant derived for this system from the data is the same (within experimental error) as the saturation rate constant obtained from the kinetic study of **4a** and diphenylacetylene to form **6a** and $Me_3SiN{=}C{=}NSiMe_3$. These findings provide additional support for a dissociative mechanistic pathway in the exchange reactions, since the rate constant in the formal [2 + 2] retrocycloaddition reaction to generate imidozirconocene species $Cp_2Zr{=}N\text{-}t\text{-}Bu$ (**7a**) and $Me_3SiN{=}C{=}NSiMe_3$ should be the same for both reactions.

Introduction

Monomeric metal imido (M=NR) complexes are now known throughout the transition-metal series. The imide linkage can be either reactive or unreactive, depending on the metal and the remaining ligand set of the complex. Unreactive organoimido ligands have served as ancillary groups in a number of organometallic compounds, such as the tungsten carbene complex **1** depicted in Figure 1, discovered by Schrock and co-workers to be an effective homogeneous catalyst for olefin metathesis.[1] Other early-metal alkylidenes with spectator imide ligands have been applied as catalysts for olefin metathesis as well as polymerization reactions.[2,3]

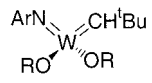

1

Ar = 2,6-^{i}Pr$_2$Ph

R = OCMe(CF$_3$)$_2$

Figure 1. Homogeneous olefin metathesis catalyst **1**.

*To whom correspondence should be addressed. E-mail: bergman@cchem.berkeley.edu.

† This paper is dedicated to Prof. Ronald Breslow on the occasion of his 70th birthday.

10.1021/om010091o CCC: $20.00
Publication on Web 04/04/2001

In addition to the large number of organometallic structures known in which the organoimido ligand is unreactive, there are a growing number of systems in which the imide linkage undergoes chemical transformation. In early-transition-metal imido complexes, the nucleophilicity of the nitrogen atom combined with the high electrophilicity of the metal center can generate high reactivity with small, unsaturated organic molecules. Some multiply bonded metal−nitrogen complexes are known for their synthetic applications as stoichiometric nitrene sources in heteroatom transfer reactions.[4,5] Additionally, metal imido complexes have been proposed as the catalytic agents in many organic transformations such as hydroamination of alkynes[6−8] and allenes,[9,10] hydrodenitrogenation,[11,12] nitrile reduction,[13−15] and the metathetical exchange between organic imines.[16−21]

Many of these reactions involve an initial overall [2 + 2] cycloaddition between the metal−nitrogen double bond and the double bond of the unsaturated organic substrate to generate a four-membered metallacycle (eq 1). The intermediacy of a metallacycle is supported by

(1)

mechanistic and kinetic studies for several systems.[10,18−21] However, there remains a paucity of mechanistic evidence in many systems for which metallacycles have been proposed as critical intermediates.

One specific case in which metallacycles have been postulated as critical intermediates is metal-catalyzed carbodiimide metathesis reactions. For example, Weiss and co-workers previously reported carbodiimide metathesis reactions catalyzed by tungsten imido complexes.[22] More recently, Birdwhistell and co-workers have published results of carbodiimide metathesis reactions that are catalyzed by vanadium imido complexes.[23] In both cases, the researchers speculate that the carbodiimides are metathesized by imido exchange through a diazametallacycle intermediate (e.g., the Weiss et al. mechanism in Scheme 1).

Scheme 1

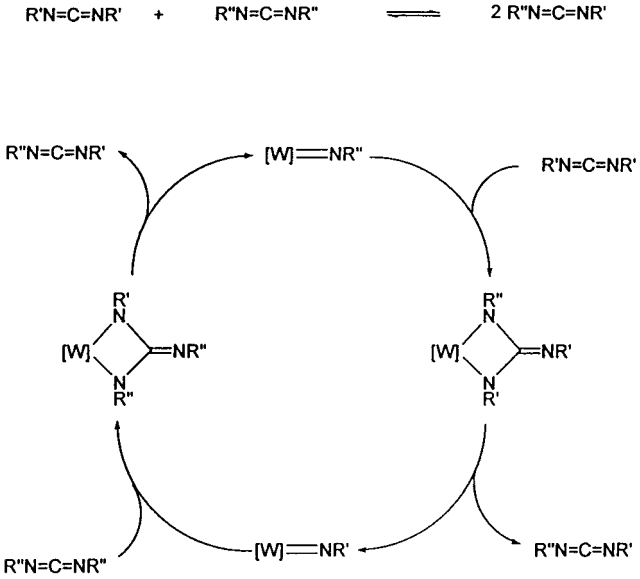

Since cycloreversion/cycloaddition reactions of transition-metal imido complexes with heterocumulenes are established or proposed fundamental steps in many processes, we have been interested in enhancing our mechanistic understanding of these reactions. Monomeric zirconocene imido complexes with the general structure $Cp_2Zr{=}NR$ react with unsaturated organic substrates (alkynes,[10,24,25] allenes,[10] imines,[18,19] azides,[19] carbodiimides,[26] etc.) to afford formal [2 + 2] cycloaddition products. Because of the thermal stability of many of these complexes, isolation and direct examination of their reactivity with unsaturated substrates can be carried out. Reported in this paper is a study of cycloreversion/cycloaddition reactions between zirconocene imido complexes and unsaturated organic molecules (alkynes and carbodiimides). Data from the kinetic analysis of several of these systems are presented.

Results

Exchange Reactions of Diazametallacycle Complexes 4a−d with Alkynes. The zirconocene diazametallacycle complexes utilized throughout this study were prepared from $Cp_2(THF)Zr{=}NR$ (R = *t*-Bu, 2,6-$Me_2C_6H_3$, 2,6-*i*-$Pr_2C_6H_3$) and 1 equiv of a symmetrical carbodiimide (R′N=C=NR′).[26] The highly colored zir-

(1) Schaverien, C. J.; Dewan, J. C.; Schrock, R. R. *J. Am. Chem. Soc.* **1986**, *108*, 2771.
(2) Ivin, K. I. *Olefin Metathesis;* Academic Press: London, 1983.
(3) Hursthouse, M. B.; Motevalli, M.; Sullivan, A. C.; Wilkinson, G. J. *J. Chem. Soc., Chem. Commun.* **1986**, 1398.
(4) (a) Wang, W.; Espenson, J. H. *Organometallics* **1999**, *18*, 5170. (b) McInnes, J. M.; Mountford, P. *Chem. Commun.* **1998**, 1669. (c) McInnes, J. M.; Blake, A. J.; Mountford, P. *J. Chem. Soc., Dalton Trans.* **1998**, 3623.
(5) Lee, S. Y.; Bergman, R. G. *J. Am. Chem. Soc.* **1996**, *118*, 6396.
(6) Haak, E.; Bytschkov, I.; Doye, S. *Angew. Chem., Int. Ed. Engl.* **1999**, *38*, 3389.
(7) McGrane, P. L.; Jensen, M.; Livinghouse, T. *J. Am. Chem. Soc.* **1992**, *114*, 5460.
(8) McGrane, P. L.; Livinghouse, T. *J. Am. Chem. Soc.* **1993**, *115*, 11485.
(9) Walsh, P. J.; Baranger, A. M.; Bergman, R. G. *J. Am. Chem. Soc.* **1992**, *114*, 1708.
(10) Baranger, A. M.; Walsh, P. J.; Bergman, R. G. *J. Am. Chem. Soc.* **1993**, *115*, 2753.
(11) Gray, S. D.; Smith, D. P.; Bruck, M. A.; Wigley, D. E. *J. Am. Chem. Soc.* **1992,** *114*, 5462.
(12) Perot, G. *Catal. Today* **1991**, *10*, 447.
(13) Bakir, M.; Fanwick, P. E.; Walton, R. A. *Inorg. Chem.* **1988**, *27*, 2016.
(14) Rhodes, L. F.; Venanzi, L. M. *Inorg. Chem.* **1987**, *26*, 2692.
(15) Han, S. H.; Geoffroy, G. L. *Polyhedron* **1988**, *7*, 2331.
(16) Cantrell, G. K.; Meyer, T. Y. *Organometallics* **1997**, *16*, 5381.
(17) Cantrell, G. K.; Meyer, T. Y. *J. Am. Chem. Soc.* **1998**, *120*, 8035.
(18) Meyer, K. E.; Walsh, P. J.; Bergman, R. G. *J. Am. Chem. Soc.* **1994**, *116*, 2669.
(19) Meyer, K. E.; Walsh, P. J.; Bergman, R. G. *J. Am. Chem. Soc.* **1995**, *117*, 974.
(20) Krska, S. W.; Zuckerman, R. L.; Bergman, R. G. *J. Am. Chem. Soc.* **1998**, *120*, 11828.
(21) Zuckerman, R. L.; Krska, S. W.; Bergman, R. G. *J. Am. Chem. Soc.* **2000**, *122*, 751.
(22) Meisel, I.; Hertel, G.; Weiss, K. *J. Mol. Catal.* **1986**, *36*, 159.
(23) Birdwhistell, K. R.; Lanza, J.; Pasos, J. *J. Organomet. Chem.* **1999**, *584*, 200.
(24) Walsh, P. J.; Hollander, F. J.; Bergman, R. G. *J. Am. Chem. Soc.* **1988**, *110*, 8729.
(25) (a) Walsh, P. J.; Hollander, F. J.; Bergman, R. G. *Organometallics* **1993**, *12*, 3705. (b) Molina, P.; Alajarin, M.; Saez, J. *Synth. Commun.* **1982**, *12*, 573.
(26) The details of the study for overall [2 + 2] cycloaddition of $Cp_2Zr{=}NR$ species with carbodiimides has been published independently: Zuckerman, R. L.; Bergman, R. G. *Organometallics* **2000**, *19*, 4795.

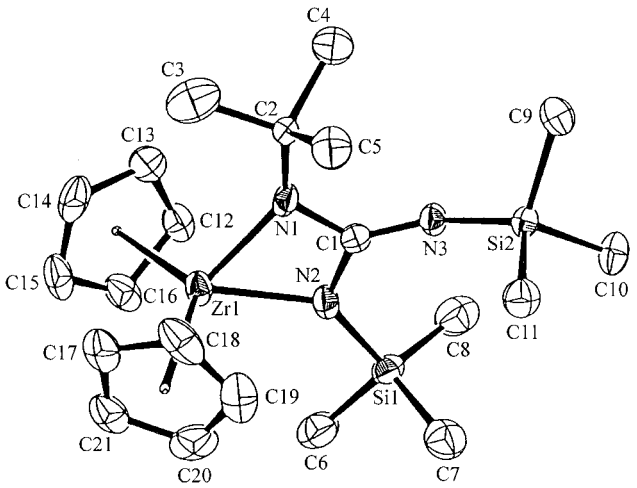

Figure 2. ORTEP diagram of **4a**. The thermal ellipsoids are scaled to represent the 50% probability surface.

conacycles generated from the reaction can be isolated in high yields after crystallization. For example, treatment of $Cp_2(THF)Zr{=}N\text{-}t\text{-}Bu$ (**2a**) with 1 equiv of $Me_3SiN{=}C{=}NSiMe_3$ (**3a**) in C_6H_6 at 25 °C gave clean conversion to the diazametallacycle complex **4a** (eq 2).

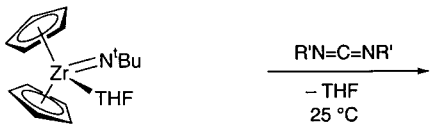

2a

3a; R' = $SiMe_3$
3b; R' = ^{t}Bu
3c; R' = ^{i}Pr
3d; R' = Cyc
3e; R' = *p*-Tol
3f; R' = *m*-Tol

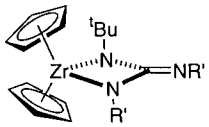

(2)

4a; R' = $SiMe_3$
4b; R' = ^{i}Pr
4c; R' = Cyc
4d; R' = *p*-Tol
4e; R' = *m*-Tol

Red X-ray-quality crystals were obtained by slow evaporation of a solution of **4a** in hexanes (45% yield). An ORTEP diagram of **4a** is shown in Figure 2. The metallacyclobutane ring of **4a** is planar; the dihedral angle between the plane formed by Zr, N1, and N2 and the plane formed by C1, N1, and N2 is 177°. The Zr–N1 and Zr–N2 bond distances are 2.117(3) and 2.1222(2) Å, respectively, and are close to those seen in several other structurally similar zirconocene amido complexes.[25,27,28] The bond lengths for N1–Cl and N2–C1 are virtually the same, 1.393(4) and 1.408(4) Å, respectively (Table 1; see Table 2 for crystallographic data). The shorter N3–Cl bond length of 1.278(4) Å indicates greater electron density in the exocyclic C–N bond of the four-membered zirconacycle.

Table 1. Selected Bond Lengths (Å) and Bond Angles (deg) for Compound 4a

Bond Lengths			
Zr1–N1	2.117(3)	Zr1–N2	2.1222(2)
Zr1–Cp1	2.2361(3)	Zr1–Cp2	2.242631)
Si1–N2	1.676(3)	C1–C2	1.435(3)
Si1–C7	1.779(4)	Si1–C6	1.789(4)
Si2–N3	1.674(2)	Si2–C9	1.884(4)
Si2–C10	1.868(4)	Si2–C11	1.877(4)
Si3–N1	1.669(3)	NI–C1	1.393(4)
N1–C2	1.429(5)	N2–C1	1.408(4)
N3–C1	1.278(4)	C2–C4	1.680(5)

Bond Angles			
N1–Zr1–N2	64.17(9)	N1–Zr1–C1	31.97(9)
N1–Zr1–Cp1	111.55(7)	N1–Zr1–Cp2	111.53(7)
N2–Zr1–C1	32.39(9)	N2–Zr1–C101	112.78(7)
N2–Zr1–Cp2	110.3(7)	C101–Zr1–Cp1	128.65(1)
N2–Si1–C6	105.5(2)	Zr1–N1–C1	159.1(2)
N2–Si1–C8	112.8(2)	N2–Si1–C7	112.1(2)
C6–Si1–C8	106.8(2)	C6–Si1–C7	108.6(2)
N3–Si2–C9	113.8(1)	N3–Si2–C10	111.8(1)
N3–Si2–C11	110.3(1)	Si3–N1–C1	126.8(2)
Zr1–N1–Si3	138.7(1)	Zr1–N2–Si1	140.2(2)
Zr1–N1–C2	138.6(2)	Si1–N2–C1	125.1(2)
C1–N1–C2	126.3(3)	N1–C1–N2	107.0(3)
Zr1–N2–C1	93.7(2)	N2–C1–N3	124.8(3)
Si2–N3–C1	154.7(2)	N1–C2–C4	110.4(3)
NI–C –N3	128.1(3)	C3–C2–C5	107.9(3)
N1–C2–C3	111.5(3)		

Table 2. Crystallographic Data for Compounds 4a and 10a

	4a	**10a**
formula	$C_{21}H_{37}N_3Si_2Zr$	$C_{49}H_{58}N_3Zr$
fw	478.93	780.24
color	orange, plate	orange, prism
cryst syst	monoclinic	monoclinic
lattice type	primitive	primitive
temp (K)	143	149
space group	$P2_1/n$ (No. 14)	$P2_1/n$ (No. 14)
a, Å	9.3306(1)	11.9802(2)
b, Å	14.3003(2)	20.9083(4)
c, Å	18.5893(1)	19.0025(4)
α, deg	90.00	90.00
β, deg	91.839(1)	98.175(1)
γ, deg	90.00	90.00
V, Å^3	2479.10(4)	4711.5(1)
Z	4	4
μ(Mo Kα) cm^{-1}	5.50	2.65
D_{calcd}, g/cm^3	1.283	1.1
total no. of data	11 855	22 126
residuals: *R*; R_w	0.034; 0.046	0.046; 0.047
GOF	1.73	1.40
radiation	Mo Kα (λ = 0.710 69 Å), graphite monochromated	

Treatment of diazametallacycle **4a** with 1 equiv of diphenylacetylene (**5a**) (Table 3) at 25 °C in C_6D_6 resulted in an immediate color change from reddish orange to forest green. Azametallacyclobutene **6a** was the organometallic product, produced in 92% yield based on an internal standard. The identity of **6a** was confirmed by comparison of its ^{1}H NMR spectroscopic data with literature values.[24] Spectroscopic data revealed that the heterocumulene $Me_3SiN{=}C{=}NSiMe_3$ (**3a**) had also formed during the course of the reaction in 98% yield.

When the analogous reaction was carried out in the presence of 2-butyne (**5b**) (Table 3), there was a color

(27) Cardin, D. J.; Lappert, M. F.; Raston, C. L. *Chemistry of Organo-Zirconium and -Hafnium Compounds;* Ellis Horwood: New York, 1986.

(28) Arney, D. J.; Bruck, M. A.; Huber, S. R.; Wigley, D. E. *Inorg. Chem.* **1992**, *31*, 3749.

Table 3. Exchange Reaction of Diazametallacycle Complexes 4a,b with Alkynes

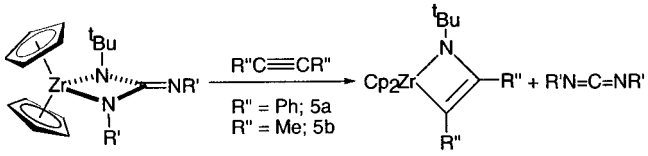

4 6 3

diaza-metallacycle reactant	R′	alkyne	metalla-cyclobutene product	carbo-diimide product	yield, % (^{1}H NMR)
4a	$SiMe_3$	**5a**	**6a**	**3a**	92
4a	$SiMe_3$	**5**	**6b**	**3a**	81
4b	*i*-Pr	**5a**	**6**	**3c**	20

change from reddish orange to blue. Similar to the previous reaction, formation of metallacyclobutene **6b** and carbodiimide **3a** was observed by ^{1}H NMR spectroscopy in 81% and 97% yields, respectively, based on an internal standard.

This alkyne/carbodiimide exchange reaction was difficult to generalize. When zirconacycle **4b** was treated with alkyne **5a** in C_6D_6, no reaction was observed at 25 °C (Table 3). Heating at 80 °C for 66 h did result in the complete consumption of zirconacycle complex **4b**, but only ca. 20% of metallacyclobutene **6a** formed, based on an internal standard, with unidentifiable impurities comprising the remaining organometallic material. When zirconacycle **4c** was heated at 80 °C in the presence of diphenylacetylene (**5a**) or 2-butyne (**2b**), only decomposition products were observed by ^{1}H NMR spectroscopy. Diazametallacycle complex **4d** was found to be more thermally robust when heated with diphenylacetylene (**5a**) or 2-butyne (**5b**) than either **4b** or **4c** and did not begin to decompose until it was heated at 135 °C for 24 h. There was no observable azametallacyclobutene **6a** or **6b** formation under the reaction conditions employed.

Kinetic Analysis of the Reaction between 4a and Alkyne 5a. The proposed mechanism of the exchange reaction between complex **4a** and diphenylacetylene (**5a**) is outlined in Scheme 2. To verify that this reaction occurs by a dissociative process, kinetic studies were carried out by monitoring the formation of metallacyclobutene complex **6a**. Applying the steady-state approximation to the concentration of intermediate **7a** predicts the rate law shown in eq 3. According to this

$$\text{rate} = k_2k_3[\mathbf{4a}][\mathbf{5a}]/(k_2[\mathbf{3a}] + k_3[\mathbf{5a}]) \qquad (3)$$

rate law, when $k_2[\mathbf{3a}] \gg k_3[\mathbf{5a}]$, the reaction will be first order in [**4a**] and [**5a**] and inverse first order in [**3a**] (eq 4). At high concentration of [**5a**], the reaction should

$$\text{rate} = k_1k_3[\mathbf{4a}][\mathbf{5a}]/(k_2[\mathbf{3a}]) \qquad (4)$$

exhibit saturation kinetics wherein the rate will be first order in [**4a**] and zero order in [**3a**] and [**5a**] (eq 5).

$$\text{rate} = k_1[\mathbf{4a}] \qquad (5)$$

Conditions for the kinetic experiments are discussed in the Experimental Section. Each run was performed with excess concentrations of carbodiimide **3a** and diphenylacetylene (**5a**) relative to the concentration of

Scheme 2

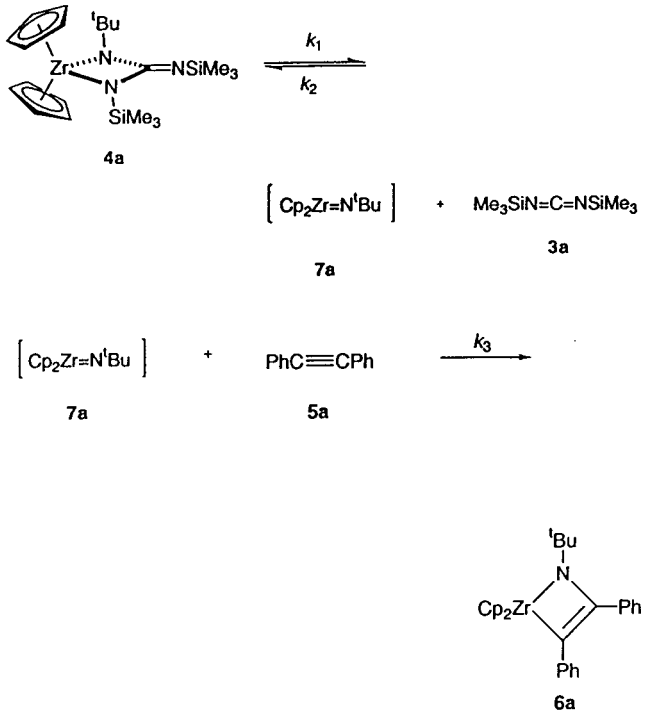

the reactant zirconacycle **4a** in C_6H_6 to ensure pseudo-first-order conditions (see Table S-11 in the Supporting Information). The absorbance of product metallacyclobutene **6a** was monitored (λ = 420 nm) by UV−vis spectroscopy at 15.4 ± 0.1 °C and plotted vs time (see Figure S-3 in the Supporting Information for a sample plot).

Excellent pseudo-first-order behavior was observed under the experimental conditions employed. Plots of the increase in [**6a**] vs time gave exponential growth consistent with the reaction being first order in [**4a**]. Rates were measured using variable excess concentrations of alkyne **5a** and carbodiimide **3a.** At lower concentrations, the rates of reaction were accelerated with added **5a** and slowed by addition of carbodiimide **3a**. At higher concentrations of **5a**, saturation kinetics were observed, as illustrated in the plot of k_{obs} vs [**3a**]/[**5a**] (Figure 3). A plot of $1/k_{obs}$ versus [**5a**]/[**3a**] (Figure 3, inset) shows a linear dependence of the ratio of alkyne to carbodiimide. The data are congruent with the rate law derived in eq 3, and the values of $k_1 = (3.3 \pm 0.1) \times 10^4$ s^{-1} and $k_3/k_2 = 0.4$ at 15.4 ± 0.1 °C are obtained from these data.

We carried out a competition experiment to independently confirm the value of k_3/k_2. The coordinatively unsaturated imidozirconocene compound **7a** is not an isolable species, but complex **2a** functions as a convenient precursor to this transient intermediate (Scheme 3). A solution of zirconocene imido complex **2a** in the presence of 10 equiv of **3a** and 10 equiv of **5a** in d_8-toluene at −78 °C was prepared. The reaction between **2a** and the unsaturated organic complexes **3a** and **5a** to generate the corresponding diazametallacycle complexes **4a** and **6a** was monitored at low temperature by ^{1}H NMR spectroscopy. The metallacycle ratio was measured from the integration of the cyclopentadienyl signals for the two corresponding organometallic com-

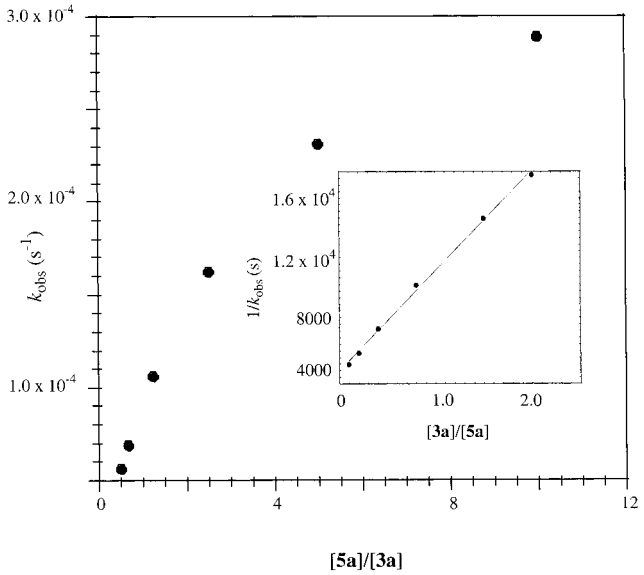

Figure 3. Plot of k_{obs} vs [**5a**]/[**3a**] for the appearance of **6a** at 15.4 ± 0.1 °C and the double-reciprocal plot of $1/k_{obs}$ vs [**3a**]/[**5a**] (inset). A linear fit gave the correlation coefficient $\gamma = 0.99$.

Scheme 3

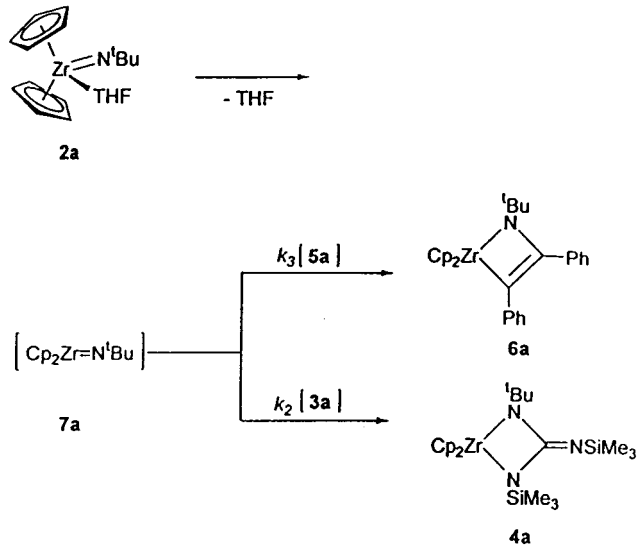

pounds (δ 5.96 for **6a** and δ 6.02 for **4a**) at −40 °C. To ensure the product ratio was being measured in the kinetic regime, monitoring of the reaction was continued while the probe of the NMR spectrometer was warmed to 25 °C. The ratio began to shift at −15 °C (**6a**:**4a** 0.67:l from **6a**:**4a** 0.4:1 at −40 °C), demonstrating the reversibility of the reaction. Complete conversion to the thermodynamic product, metallacyclobutene **6a**, was obtained by the time the probe was warmed to 25 °C. Measuring the ratio of metallacycle complexes **4a** and **6a** generated under kinetic conditions and dividing out the concentrations gave a k_3/k_2 value of 0.4 ± 0.04 at −40 °C. This is in good agreement with the experimentally derived value of $k_3/k_2 = 0.4 \pm 0.01$ at 15.4 ± 0.1 °C from the kinetic analysis.

Exchange Reactions of Diazametallacycle Complexes 8a−d with Alkynes. Since the N−R substituents from the parent carbodiimide fragment of zirconocene diazametallacycle complexes **4a−d** were found to have a substantial influence on the rate of exchange between **4** and alkynes, we wanted to determine whether the substituent on the imido nitrogen would have a similarly strong effect. We therefore prepared the aryl-substituted diazametallacycle complex **8a** with a procedure analogous to that used for the generation and isolation of diazametallacycle complexes **4a−e** (eq 6) and

Table 4. Exchange Reaction of Diazametallacycle Complexes 8a,b with Alkynes

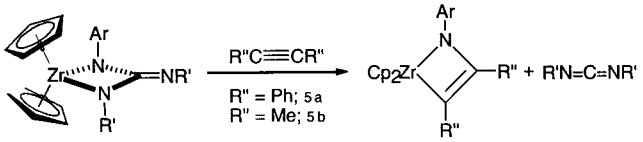

diaza-metallacycle reactant	R′	alkyne	metalla-cyclobutene product	carbo-diimide product	yield, % (^{1}H NMR)
8a	$SiMe_3$	**5a**	**6c**	**3a**	100
8a	$SiMe_3$	**5b**	**6d**	**3a**	93
8b	*t*-Bu	**5a**	**6c**	**3b**	98

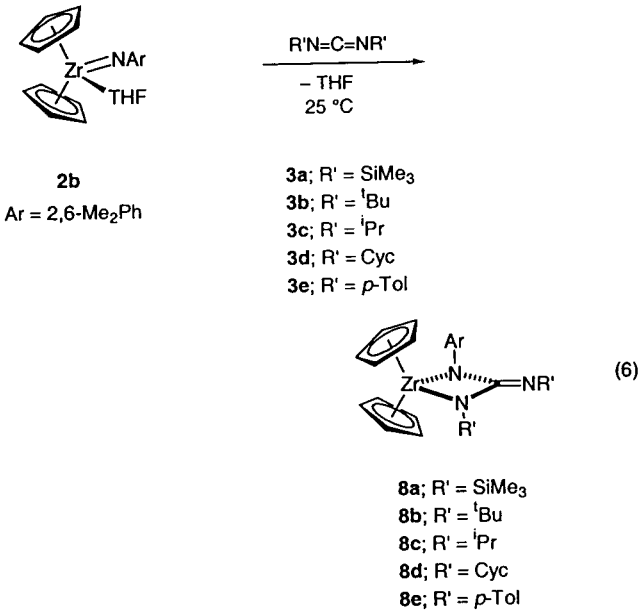

examined the reaction of **8a** with diphenylacetylene (**5a**). Treatment of zirconacycle **8a** in C_6D_6 with 1 equiv of **5a** (Table 4) resulted in an immediate color change to green from red. The ^{1}H NMR spectroscopic data showed the disappearance of free diphenylacetylene and a shift in the resonance for the cyclopentadienyl ligands of **8a** from δ 6.96 to 5.83. There was virtually no change in the chemical shift for the methyl groups on the aromatic ring (δ 2.19), but the two Me_3Si resonances of zirconacycle **8a** (δ 0.32 and 0.06) were no longer present. A resonance corresponding to the methyl groups of free $Me_3SiN{=}C{=}NSiMe_3$ (**3a**) at δ 0.1 was observed. The organometallic product was confirmed to be diazametallacyclobutene **6c** by comparison of spectroscopic data with literature values for **6c**.[24] Similar to the reaction of **4a** and 2-butyne to generate metallacyclobutene **6b**, metallacycle **8a** also reacted with 2-butyne to generate azametallacyclobutene **6d** (Table 4) with the concurrent release of carbodiimide **3a**.

Scheme 4

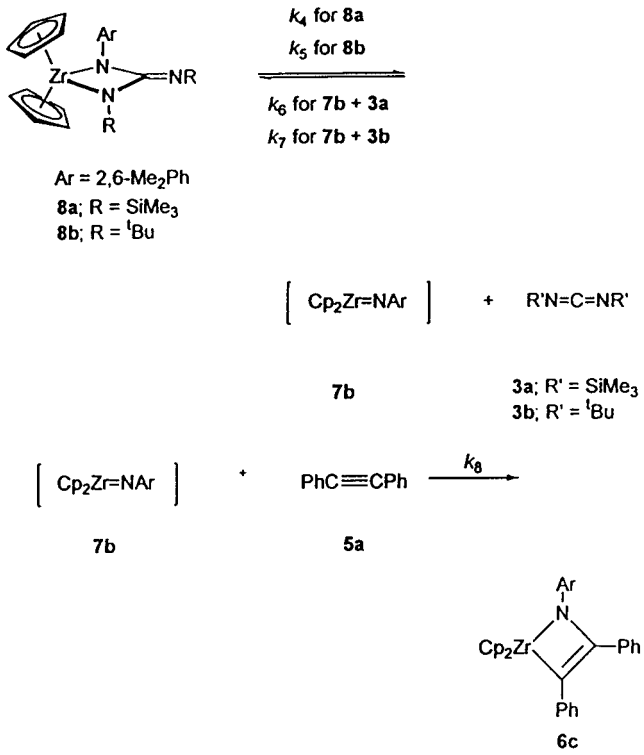

Analogous exchange reactivity was observed between diazametallacycle **8b** and diphenylacetylene to cleanly form metallacyclobutene **6c** and (*t*-Bu)N=C=N(*t*-Bu) (**3b**) (Table 4). Reaction of **8b** with 2-butyne (**5b**) gave an immediate reaction at 25 °C, demonstrated by an instantaneous color change from purple to blue upon mixing the two reactants. The organometallic product was identified as **6d** by comparison of spectroscopic data with literature values for **6d**.[24] When zirconacycles **8c**−**e** were treated with either diphenylacetylene or 2-butyne, there was no observable exchange reaction. Upon further heating at elevated temperatures, only thermal decomposition products were observed.

Kinetic Analysis of the Reaction between 8a and Alkyne 5a. Comparing the reactions of the two diazametallacycle complexes **4a** and **8a** in the exchange with alkyne **5a**, we noted qualitatively an increase in the rate of metallacyclobutene formation with the reactant **8a**. For this reason, we decided to determine whether the mechanistic pathway for the exchange reaction of **8a** with diphenylacetylene was a dissociative process, as in the case of **4a** and **5a** (Scheme 2). If this system follows a similar mechanism (Scheme 4), we would be able to study the effect of the N-alkyl group on reaction rate. This information should facilitate our understanding of substituent effects in the cycloreversion/cycloaddition of zirconocene imido complexes and alkyne **5a**.

Accordingly, metallacycle **8a** was treated with 10 equiv of **3a** and **5a** at 25 °C in C_6D_6, and the reaction was monitored by ^{1}H NMR spectroscopy. Under these conditions, azametallacyclobutene complex **6c** was cleanly formed with no observable impurities. Using UV−vis spectroscopy, several kinetic runs were performed in C_6H_6 with excess concentrations of $Me_3SiN{=}C{=}NSiMe_3$ (**3a**) and diphenylacetylene (**5a**) relative to the concentration of the limiting reactant zirconacycle **8a** to ensure pseudo-first-order conditions (see Table S-12 in the Supporting Information). The appearance of product metallacyclobutene **6c** was monitored at 5.0 ± 0.1 °C by UV−vis spectroscopy, and rate data were collected over four half-lives at $\lambda = 550$ nm.

A plot of [**6c**] vs time gave exponential growth indicative of a pseudo-first-order reaction. The reaction was first order in [**8a**] but zero order in [**5a**], even at the lowest concentrations of this reactant that we were conveniently able to reach while still maintaining pseudo-first-order conditions in [**8a**]. Two runs were carried out with no added **3a** while the concentration of added **5a** was varied to ensure that we achieved saturation in the reactions with added **3a**. The k_{obs} values for both of these reactions were virtually the same. These data (see Table S-12 in the Supporting Information) are consistent with the rate law described in eq 7, with $k_4 = (2.3 \pm 0.02) \times 10^{-3}$ s^{-1}. For this

$$\text{rate} = k_4k_8[\mathbf{8a}][\mathbf{5a}]/(k_6[\mathbf{3a}] + k_8[\mathbf{5a}]) \qquad (7)$$

system, k_8/k_6 could not be obtained from the kinetic study due to the inaccessibility of the region in which $k_6[\mathbf{3a}] \gg k_8[\mathbf{5a}]$.

Kinetic Analysis of the Reaction between Diazametallacycle Complex 8b and Alkyne 5a. We extended the above study by examining the mechanism of the alkyne exchange reaction between metallacycle **8b** and alkyne **5a** (Scheme 4). Similar results were obtained when kinetic studies were performed on this analogous system, again utilizing a large excess of added carbodiimide **3b** and **5a** relative to the concentration of metallacycle **8b**. The rate and concentration data are listed in Table S-13 in the Supporting Information. The data obtained for this system were consistent with the rate law given in eq 8, but once again only the regime

$$\text{rate} = k_5k_8[\mathbf{8b}][\mathbf{5a}]/(k_7[\mathbf{3b}] + k_8[\mathbf{5a}]) \qquad (8)$$

in which $k_8[\mathbf{5a}] \gg k_7[\mathbf{3a}]$ could be accessed (i.e., the reaction was zero-order in [**5a**]). The experimentally derived value of $k_5 = (2.00 \pm 0.02) \times 10^{-3}$ s^{-1} was obtained. Unfortunately, when we increased the concentration of added carbodiimide **3b** in order to access the region in which $k_7[\mathbf{3a}] \gg k_8[\mathbf{5a}]$, side reactions occurred that prevented the collection of reliable kinetic data.

Insertion Reactions of Diazametallacycle Complexes 9a−d with Diphenylacetylene. Different chemistry is observed when alkynes are allowed to react with metallacycles that contain bulkier ortho substituents on the phenyl ring. From previous studies of the formal [2 + 2] cycloaddition reactions between zirconocene imido complexes with carbodiimides, we knew that **2c** does not react with $Me_3SiN{=}C{=}NSiMe_3$ or (*t*-Bu)N=C=N(*t*-Bu), even at elevated temperatures. However, metallacycle complexes **9a**,**b** can be isolated in high yields from the overall cycloaddition between **2c** and CycN=C=NCyc (**3d**) and (*i*-Pr)N=C=N(*i*-Pr) (**3c**), respectively (Scheme 5).[26] Diazametallacycle **9a** was treated with 1 equiv of alkyne **5a** at 25 °C in C_6D_6. No observable reaction took place until the mixture was heated to 75 °C, upon which a color change from purple to orange occurred. Analysis of the reaction mixture by ^{1}H NMR spectroscopy revealed a new organometallic product had cleanly formed that incorporated 1 equiv

Scheme 5

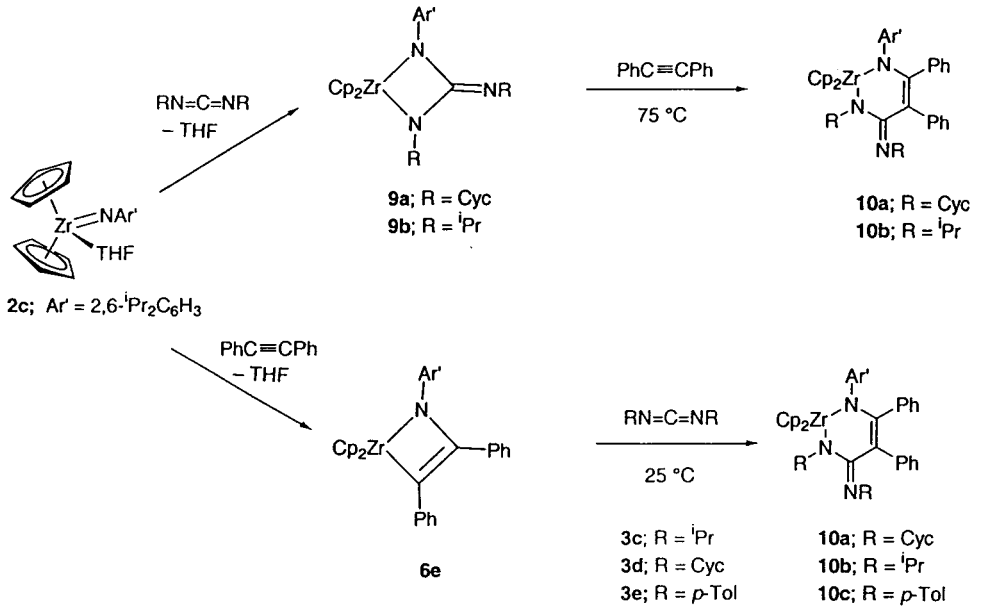

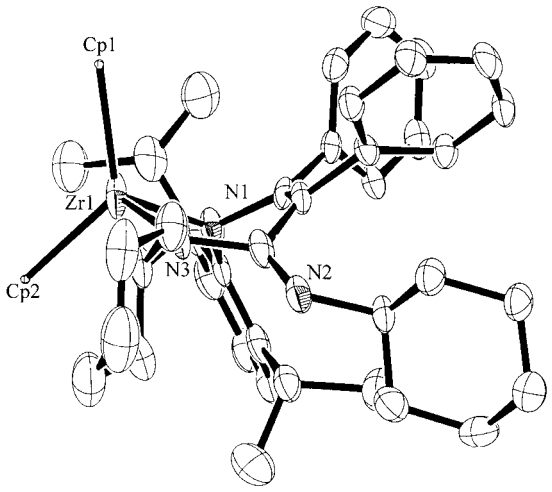

Figure 4. ORTEP diagram of **10a**. The thermal ellipsoids are scaled to represent the 50% probability surface.

Table 5. Selected Bond Lengths (Å) and Bond Angles (deg) for Compound 10a

Bond Lengths			
Zr1−N1	2.117(4)	Zr1−N3	2.126(4)
Zr1−Cp1	2.2949(6)	Zr1−Cp2	2.1437(6)
N1−C11	1.438(8)	N1−C14	1.453(6)
N2−C13	1.299(6)	N2−C38	1.475(6)
N3−C13	1.495(6)	N3−C44	1.481(7)
C11−C12	1.363(7)	C11−C26	1.500(7)
C12−C13	1.503(7)	C12−C32	1.515(7)
C14−C15	1.409(7)	C15−C20	1.509(8)
C16−C17	1.378(8)	C17−C18	1.375(8)
C18−C19	1.395(7)	C23−C25	1.554(7)
C20−C21	1.528(9)		
Bond Angles			
N1−Zr1−N3	91.6(2)	N1−Zr1−Cp1	115.3(1)
N1−Zr1−Cp2	103.3(1)	N3−Zr1−Cp1	106.9(1)
Cp1−Zr1−Cp2	126.60(2)	Zr1−N1−C11	108.3(3)
Zr1−Ni−C14	136.7(3)	N1−C10−C5	116.7(2)
N1−Zr1−C8	103.0(2)	C11−N1−C14	114.8(4)
C13−N2−C38	123.1(5)	Zr1−N3−C13	117.1(3)
Zr1−N3−C44	125.3(3)	C13−N3−C44	117.2(4)
N3−Zr1−C2	81.5(2)	N1−C11−C26	116.5(4)
C11−C12−C13	127.0(4)	C13−C12−C32	113.2(4)
N2−C13−C12	124.7(4)	N1−C14−C15	121.0(5)
C15−C14−C19	120.4(5)	C17−C18−C19	121.6(6)
C14−C19−C23	122.8(5)	C15−C20−C21	112.2(5)
N2−C38−C39	106.7(4)	N3−C44−C45	113.7(4)

of **5a**. Unlike the exchange reactivity seen between zirconocene diazametallacycle complexes **4a**,**b** and **8a**,**b** and alkynes, there was no evidence of free carbodiimide being formed during the course of the reaction. Additionally, the product exhibited two resonances in the cyclopentadienyl region of the ^{1}H NMR spectrum (δ 6.43 and 5.02), each integrating to five hydrogens. Repeating the reaction on a preparative scale resulted in the isolation of an orange solid; crystallization from hexanes provided pure material in 65% yield. An ORTEP diagram obtained from an X-ray diffraction study (Figure 4) showed the complex to have structure **10a**, formed by overall insertion of diphenylacetylene into the ArN−C bond of diazametallacycle complex **9a**. The metallacycle ring is in a twist-boat conformation, as is expected for an unsaturated six-membered ring with bulky substituents. The N3−C13 bond distance of 1.405(6) Å is significantly longer than the N2−C13 bond distance of 1.299(6) Å, which clearly shows substantial double-bond character between the atoms N2 and C13 (Table 5; see Table 2 for crystallographic data on **10a**). Double-bond character is also observed between the atoms C11 and C12 with a bond distance of 1.363(7) Å.

Treatment of zirconacycle **9b** with 1 equiv of diphenylacetylene yielded similar results. There was no reaction until the temperature reached 75 °C, which caused a color change from purple to yellow. Spectroscopic analysis by ^{1}H NMR showed the clean conversion to one new organometallic product that contained diastereotopic Cp resonances at δ 6.35 and 5.92. The reaction was carried out on a preparative scale in C_6H_6 to give a yellow, viscous oil. This material gave yellow crystals in 71% yield from Et_2O at −35 °C and has been fully characterized as the six-membered zirconacycle **10b**.

We obtained an interesting result when we reversed the order of addition of the reagents. Imido complex **2c** was treated with a stoichiometric amount of dipheny-

lacetylene to afford an immediate color change from yellow to forest green at 25 °C (Scheme 5). Removal of the solvent followed by crystallization from Et_2O at −35 °C gave green crystals (77% yield). This complex has been fully characterized as azametallacyclobutene **6e**. When **6e** was treated with the symmetrical carbodiimide CycN=C=NCyc (**3d**) in C_6H_6, the solution turned from green to orange over the course of 1 h at 25 °C. Analysis of the ^{1}H NMR spectrum revealed that the product formed under these conditions was **10a**, identical with the complex generated from the reaction of **9a** with diphenylacetylene at 75 °C.

This reaction was found to be general for the carbodiimide substrates tested (Scheme 5). Reaction of **6e** with 1 equiv of RN=C=NR (R = *i*-Pr, *p*-Tol) resulted in clean conversion to the corresponding six-membered-ring complexes **10b**,**c** in high yields.

Kinetic Analysis of the Reaction between 6e and 1,3-Diisopropylcarbodiimide (3c). Because of its rapid rate, we suspected an associative mechanism for the above class of reactions, involving direct insertion of an unsaturated nitrogen−carbon moiety of the carbodiimide into the zirconium−carbon bond (eq 9). If this

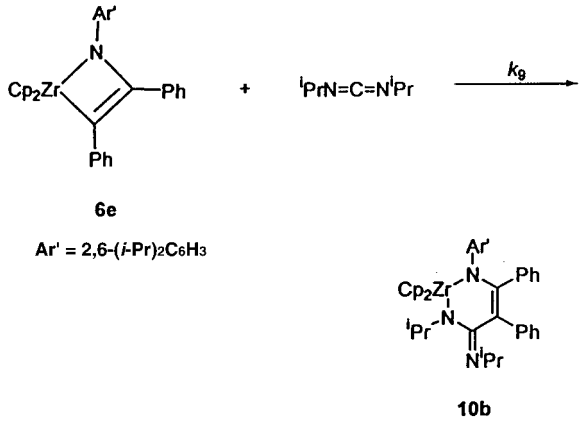

(9)

mechanistic pathway is operative for the formation of zirconacycle **10b**, the rate should be second order overall, first order in the concentration of **6e**, and first order in the concentration of carbodiimide **3c** (eq 10).

$$\text{rate} = k_9[\mathbf{6e}][\mathbf{3c}] \qquad (10)$$

The reaction was run under pseudo-first-order conditions, with concentrations of (*i*-Pr)N=C=N(*i*-Pr) (**3c**) maintained in 10-fold excess or greater relative to the concentration of metallacyclobutene **6e** (see Table S-14 in the Supporting Information for rate and concentration data for individual kinetic runs). The rate of disappearance of [**6e**] vs time showed exponential decay for **6e**. Data were taken for over 11 half-lives. A plot of k_{obs} vs [**3c**] was obtained (Figure 5) and shows a linear dependence on carbodiimide concentration **3c**, with no sign of saturation at high concentration. These data are consistent with an associative mechanism in which there is a first-order rate dependence on the concentration of metallacycle **6e** and carbodiimide **3c**. A value of $k_9 = (1.9 \pm 0.1) \times 10^{-1}$ M^{-1} s^{-1} at 15.4 ± 0.1 °C was derived from the experimental data.

Further Insertion Reactions of Azametallacyclobutene Complexes 6a,c with (*p*-Tol)N=C=N(*p*-Tol). We were curious about the cause of the different

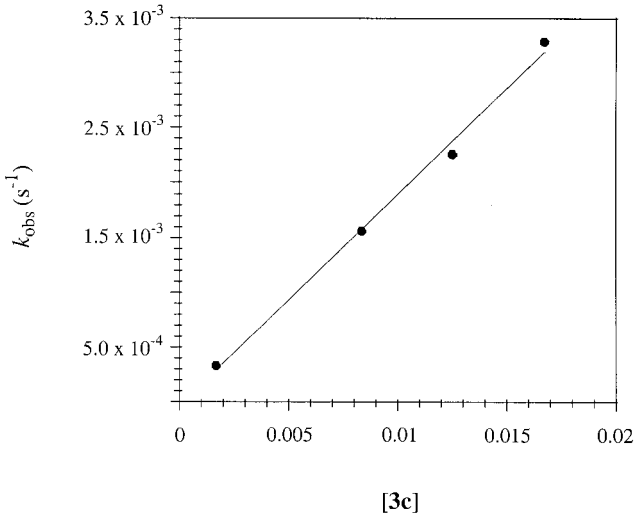

Figure 5. Plot of k_{obs} vs [**3c**] for the disappearance of **6e** at 15.4 ± 0.1 °C. A linear fit gave the correlation coefficient $\gamma = 0.99$.

reactivities observed with diazametallacycle complexes **9** and diphenylacetylene to give zirconium-containing six-membered rings vs the reactivity examined with zirconacycles **4a** and **8a**,**b** with diphenylacetylene (**5a**) and 2-butyne (**5b**). In the latter cases, only exchanges of the alkyne with the symmetrical carbodiimide component of the metallacycles to generate azametallacyclobutene complexes **6a** (Table 3) and **6c** (Table 4) were observed. Additionally, there was no evidence for further insertion of the released carbodiimides into the zirconium−carbon bond of the product metallacyclobutene complexes, unlike the reaction of **6e** with symmetrical carbodiimides (Scheme 5). To further probe the nature of the insertion reaction, we treated azametallacyclobutene complex **6a** with 1 equiv of (*p*-Tol)N=C=N(*p*-Tol) (**3e**) in the presence of $Me_3SiN=C=NSiMe_3$ at 25 °C in C_6D_6 (eq 11). The solution turned from green to

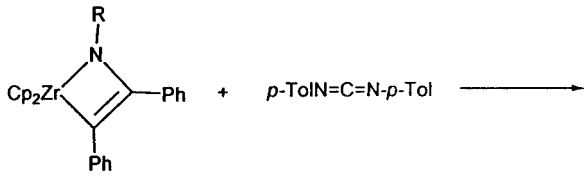

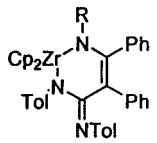

(11)

orange over 30 min. Analysis of the reaction mixture by ^{1}H NMR spectroscopy revealed two new distinct cyclopentadienyl signals, each integrating to five hydrogens, and the incorporation of (*p*-Tol)N=C=N(*p*-Tol) into the organometallic product. The reaction was repeated on a preparative scale to give zirconacycle **11** as an orange powder in 97% yield.

Table 6. Exchange Reaction of Diazametallacycle Complexes 4a and 8a with Carbodiimides

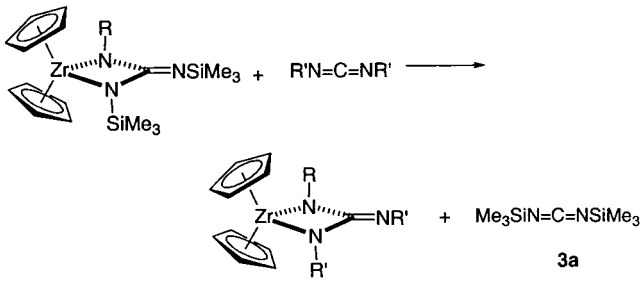

reactant diaza-metallacycle	R	R′	reactant carbo-diimide	product diaza-metallacycle	yield, % (^{1}H NMR)
4a	*t*-Bu	*i*-Pr	**3c**	**4c**	92
4a	*t*-Bu	Cyc	**3d**	**4d**	95
4a	*t*-Bu	*p*-Tol	**3e**	**4e**	97
4a	*t*-Bu	*m*-Tol	**3f**	**4f**	100
8a	2,6-Me_2Ph	*i*-Pr	**3c**	**8c**	97
8a	2,6-Me_2Ph	Cyc	**3d**	**8d**	100
8a	2,6-Me_2Ph	*p*-Tol	**3e**	**8e**	87

We next extended our investigation of carbodiimide insertion into zirconacyclobutene complexes to **6c**, the aryl analogue of **6a**. Treatment of **6c** with 1 equiv of (*p*-Tol)N=C=N(*p*-Tol) (**3e**) in the presence of Me_3SiN=C=$NSiMe_3$ (**3a**) gave results similar to those obtained when **6a** was treated with (*p*-Tol)N=C=N(*p*-Tol) (eq 11). An orange color developed over time, and spectroscopic analysis showed the split Cp resonances characteristic of all the carbodiimide-inserted products prepared in this study. Organometallic complex **12** was formed in 90% NMR yield based on an internal standard. Mass spectroscopic analysis of the mixture showed a molecular ion corresponding to the molecular weight of **12**. Treatment of **6c** with (*p*-Tol)N=C=N(*p*-Tol) in the presence of (*t*-Bu)N=C=N(*t*-Bu) (**3b**) also gave only complex **12** (^{1}H NMR spectroscopy).

Exchange Reactions of Diazametallacycle Complexes 4a and 8a with Symmetrical Carbodiimides. We pursued the study of exchange reactions between diazametallacycle complexes and other symmetrical carbodiimides (Table 6) in order to gain further mechanistic insight into the factors that govern cycloreversion/cycloaddition transformations of these complexes with unsaturated organic substrates. Treatment of diazametallacycle **4a** with 1 equiv of 1,3-di-*p*-tolylcarbodiimide (**3e**) resulted in a color change from reddish orange to blue within several hours at 25 °C. Spectroscopic analysis (^{1}H and ^{13}C NMR) confirmed that the resulting products formed from this reaction were the previously characterized zirconacycle **4d**[26] and Me_3-SiN=C=$NSiMe_3$ (**3a**). Similar results were obtained with carbodiimides **3c**,**d** (Table 6). In both of these cases, the reaction mixture turned from reddish orange to purple within hours to generate diazametallacycle complexes **4c**,**d** with the concomitant formation of carbodiimide **3a**.

Extending this study, treatment of **8a** with 1 equiv of diarylcarbodiimide **3e** resulted in the release of carbodiimide **3a** with the simultaneous formation of **8e** in 87% ^{1}H NMR yield (Table 6). It is interesting to note that the reaction proceeded more quickly than the reaction of **4a** and **3e**. Carbodiimide exchange was also observed when the reactant carbodiimide was **3c**,**d**. The solution turned from red to purple during both of these reactions, and an evaluation of the resulting mixtures by ^{1}H NMR spectroscopy confirmed clean conversion to the zirconium-containing diazacyclobutane complexes **8c**,**d**, respectively.

Scheme 6

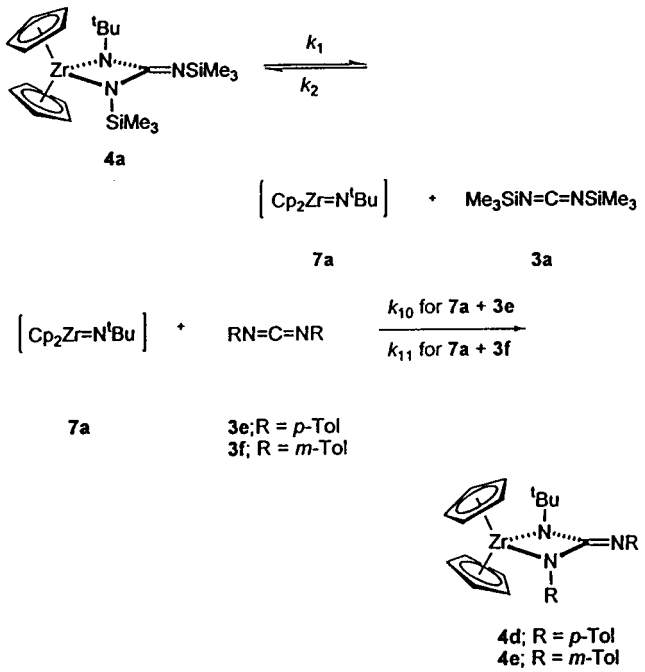

Kinetic Analysis of the Reaction between 4a and the Symmetrical Aryl Carbodiimides 3e,f. To better understand the mechanistic pathway involved in these reactions, we undertook kinetic studies of the reaction between metallacycle **4a** and carbodiimide **3e** using UV−vis spectroscopy. Outlined in Scheme 6 is the mechanistic model used for our kinetic analysis; the corresponding rate expression is given in eq 12. Conditions for the kinetic experiments are discussed in the Experimental Section. We initially attempted to hold the concentrations of added Me_3SiN=C=$NSiMe_3$ (**3a**) and (*p*-Tol)N=C=N(*p*-Tol) (**3e**) at 10-fold excess or greater relative to the concentration of **4a** to ensure pseudo-first-order conditions in the disappearance of **4a**. However, this was frustrated by the lack of solubility of carbodiimide **3e** in C_6H_6. We therefore decided to modify the study by employing carbodiimide **3e** as the limiting reactant and using concentrations of diazametallacycle **4a** and **3a** in a minimum of 10-fold excess relative to the concentration of **3e**. This gives the rate expression that is depicted in eqs 13 and 14. Table S-15

$$\text{rate} = k_1k_{10}[\mathbf{4a}][\mathbf{3e}]/(k_2[\mathbf{3a}] + k_{10}[\mathbf{3e}]) \quad (12)$$

$$\text{rate} = k_{obs}[\mathbf{3e}] \quad (13)$$

$$k_{obs} = k_1k_{10}[\mathbf{4a}]/(k_2[\mathbf{3a}] + k_{10}[\mathbf{3e}]) \quad (14)$$

in the Supporting Information contains the concentration and rate data for the individual kinetic runs. Excellent pseudo-first-order behavior was observed for this system.

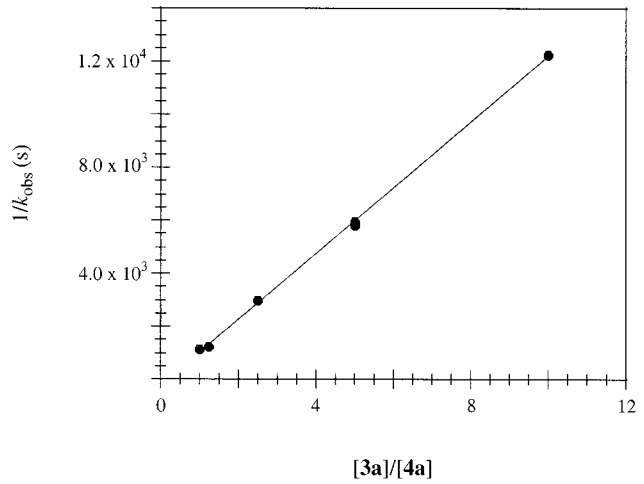

Figure 6. Plot of $1/k_{obs}$ vs [**3a**]/[**4a**]. A linear fit gave the correlation coefficient $\gamma = 0.99$.

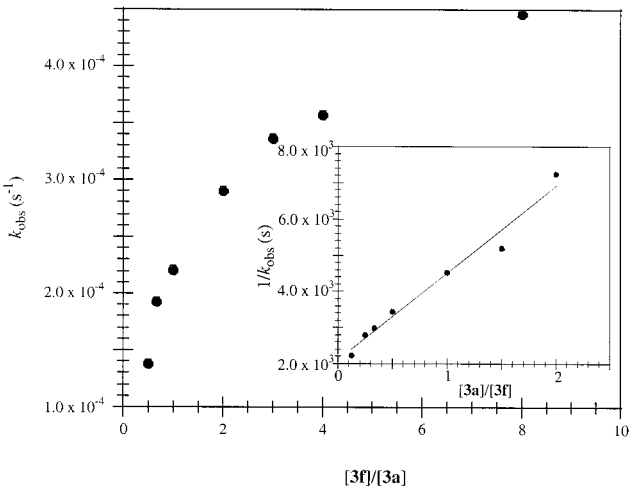

Figure 7. Plot of k_{obs} vs [**3f**]/[**3a**] for the appearance of **4e** at 15.4 ± 0.1 °C and the double-reciprocal plot of $1/k_{obs}$ vs [**3a**]/[**3f**] (inset). A linear fit gave the correlation coefficient $\gamma = 0.99$.

Plots of the increase in [**4d**] vs time gave exponential growth consistent with the reaction being first order in [**3e**]. Rates measured using variable concentrations of both **4a** and **3a** demonstrated that, under conditions where k_2[**3a**] ≫ k_{10}[**3e**], the rate was accelerated by added **4a** and inhibited by added carbodiimide **3a** (eq 15). A plot of $1/k_{obs}$ versus [**3a**]/[**4a**] shows a linear

$$k_{obs} = k_1 k_{10}[\mathbf{4a}]/(k_2[\mathbf{3a}]) \qquad (15)$$

dependence on the carbodiimide/metallacycle ratio (Figure 6). The experimentally derived value for the rate constant ratio $k_2/k_{10}k_1$ is (8.1 ± 0.1) × 10^3 s^{-1} (Scheme 6).

We next replaced carbodiimide **3e** with an analogue, 1,3-di-*m*-tolylcarbodiimide (**3f**) (Scheme 6); the rate expression for this system is outlined in eq 16. In this

$$\text{rate} = k_1 k_{11}[\mathbf{4a}][\mathbf{3f}]/(k_2[\mathbf{3a}] + k_{11}[\mathbf{3f}]) \qquad (16)$$

case, there were no observable solubility problems during our analysis by UV−vis spectroscopy, even at higher concentrations of **3f**. We were able to conveniently use excess concentrations of added **3a**,**f** relative to the concentration of metallacycle complex **4a**. Individual kinetic runs were carried out at 15.4 ± 0.1 °C, and rate data were taken for over six half-lives. Rate and concentration data for the kinetic runs carried out during the study are listed in Table S-16 in the Supporting Information. A plot of k_{obs} versus [**3f**]/[**3a**] was obtained (Figure 7). An inverse plot of $1/k_{obs}$ vs [**3a**]/[**3f**] (Figure 7, inset) shows a linear dependence on the carbodiimide concentration ratio.

These data are once again consistent with a dissociative mechanism (Scheme 6) and the rate law given in eq 16. Values of $k_1 = (4.82 \pm 0.02) \times 10^{-4}$ s^{-1} and $k_2/k_{11} = 0.8$ were derived from the inverse first-order plot. The back-reaction corresponding to the trapping of zirconocene imido complex **7a** by carbodiimide **3a** is faster than the reaction with 1,3-di-*m*-tolylcarbodiimide (**3f**) to generate the thermodynamically favored product **4e**.

Imido Group Transfer. We wanted to examine the relative thermodynamic stability of zirconocene imido complexes and the corresponding diazametallacycle complexes. Greater insight into the significant factors influencing the retrocycloaddition reaction to generate the transient imidozirconocene complexes **7** with the release of free carbodiimide might help to determine why only certain N−R imido compounds are formed. For example, the exchange reactions observed with diazametallacycle complexes **8a**,**b** with alkynes resulted in azametallacyclobutene complex **6c**,**d**, depending on the alkyne (Table 4). Treatment of Cp_2(THF)Zr=N(*t*-Bu) (**2a**) with 1 equiv of diazametallacycle **8a** in C_6D_6 at 25 °C resulted in the quantitative formation of Cp_2(THF)-Zr=N(2,6-Me_2Ph) (**2b**) and diazametallacycle complex **4a** (eq 17).

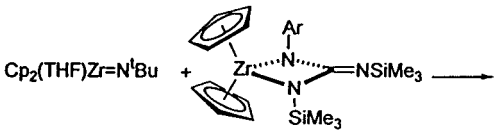

2a **8a**; Ar = 2,6-Me_2Ph

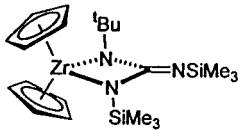

+ Cp_2(THF)Zr=NAr (17)

4a **2b**; Ar = 2,6-Me_2Ph

Discussion

Exchange Reactions of Diazametallacycle Complexes 4a and 8a,b with Alkynes. The results reported here provide mechanistic insight into the cycloreversion/cycloaddition processes of Cp_2Zr=NR species with heterocumulenes, transformations critical for several imidozirconocene-mediated stoichiometric and catalytic processes.[5,10,18−21,29,30] As shown in Table 3, when zirconacycle **4a** was treated with alkyne **5a**, metallacyclobutene complex **6a** formed cleanly with the concurrent release of carbodiimide **3a**. We considered two possible pathways for this reaction. The first is an associative process wherein diphenylacetylene (**5a**) ini-

(29) Lee, S. Y.; Bergman, R. G. *J. Am. Chem. Soc.* **1995**, *117*, 5877.
(30) Lee, S. Y.; Bergman, R. G. *Tetrahedron* **1995**, *51*, 4255.

tially reacts with **4a**. This reaction would follow a rate law that is overall second order: first order in [**4a**] and first order in [**5a**]. The second is the dissociative process outlined in Scheme 2. This begins with initial overall [2 + 2] retrocycloaddition of **4a** to generate the coordinatively unsaturated zirconocene imido complex **7a** with the release of the symmetrical carbodiimide **3a**. Imidozirconocene **7a** can be trapped by either **3a** to regenerate the starting zirconacycle or by **5a** to form azametallocyclobutene complex **6a**.

Applying the steady-state approximation to the concentration of imidozirconocene **7a** gives the rate expression that is shown in eq 3. The experimental rate data obtained fit this rate law and thus support the dissociative pathway depicted in Scheme 2. The rate constant ratio $k_2/k_1k_3 = (7.5 \pm 0.2) \times 10^3\ s^{-1}$ was obtained from the plot of $1/k_{obs}$ vs [**3a**]/[**5a**] (Figure 3, inset). The derived rate constant for the initial cycloreversion of **4a** to yield transient imidozirconocene **7a** and the released carbodiimide **3a** was experimentally determined to be $k_1 = (3.3 \pm 0.1) \times 10^{-4}\ s^{-1}$ at 15.4 ± 0.1 °C. Once **7a** forms, the rate of trapping with **3a** to regenerate **4a** is 2.5 times faster than the rate of trapping **7a** with **5a** to produce azametallacyclobutene **6a** ($k_3/k_2 = 0.4$).

Acquisition of rate data for the exchange reaction between zirconacycle **8a** and **5a** (Table 4) allows for the comparison with rate data obtained for the system of **4a** and alkyne **5a** to afford the corresponding azametallacyclobutene complex **6a** and symmetrical carbodiimide **3a** (Table 3). The only structural difference between these two systems is the parent imido substituent (*t*-Bu for **4a** and 2,6-Me_2Ph for **8a**). There were several notable differences between these two systems. For example, the reaction between **8a** and **5a** was too fast to monitor at 15.4 °C by UV−vis spectrometry. The enhanced rate for this system necessitated that the study be carried out at 5.0 ± 0.1 °C in order to obtain rate data for >4 half-lives. The reaction was determined to be first order in [**8a**] but zero order in [**5a**] even at the lowest concentrations of the latter reactant that we were conveniently able to reach while still maintaining pseudo-first-order conditions in [**8a**]. These data (Table S-12 in the Supporting Information) are consistent with the mechanism in Scheme 6 and the rate law described in eq 8. The rate constant for the cycloreversion of **8a** to give **7b** and **3a** ($k_4 = (2.3 \pm 0.02) \times 10^{-3}\ s^{-1}$ at 5.0 ± 0.1 °C) is an order of magnitude greater than the rate constant for the unimolecular cycloreversion of **4a** to generate **7a** and **3a** ($k_1 = (3.3 \pm 0.1) \times 10^{-4}\ s^{-1}$ at 15.4 ± 0.1 °C). It is difficult to say whether this effect should be attributed to a ground-state destabilization of the metallacycle caused by replacing the *t*-Bu substituent on the imido nitrogen with a di-ortho-substituted aryl moiety or if the increased rate of reversion results from stabilization of the transition state leading from **8a** to **7b**. Unfortunately, k_8/k_6 for this system could not be obtained from the kinetic study due to the inaccessibility of the kinetic region where k_6[**3a**] ≫ k_8[**5a**].

We next examined a system in which the parent carbodiimide component of the zirconacycle was varied while retaining the nitrogen-containing aromatic substituent from the parent imidozirconocene complex **2b**. Kinetic analysis of the exchange reaction between **8b** and alkyne **5a** to produce azametallacyclobutene **6c** and

Scheme 7

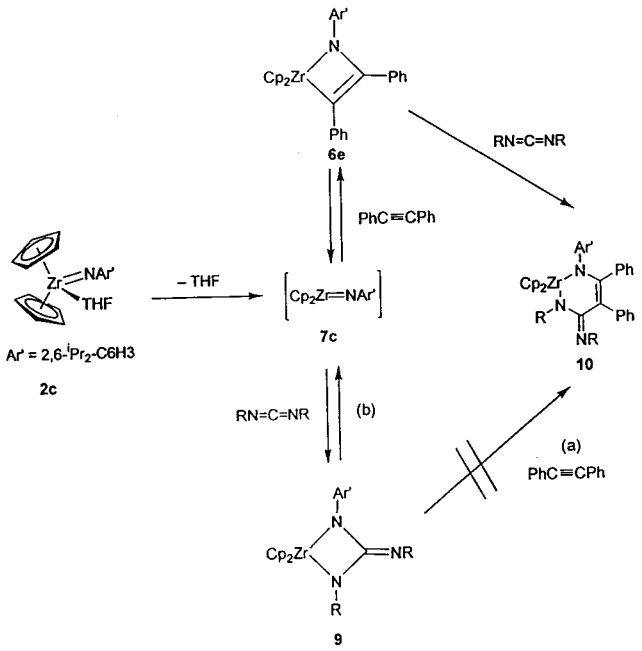

the symmetrical carbodiimide (*t*-Bu)N═C═N(*t*-Bu) (Table 4) was consistent with the dissociative mechanism outlined in Scheme 4. As in the above reactions, the transformation was determined to be first order in [**8b**] but zero order in [**5a**]. Under all conditions employed, the rate-determining transition state was found to be that for retrocycloaddition of the reactant diazametallacycle **8b** to generate imidozirconocene complex **7b** and the released carbodiimide **3b**. Because subsequent trapping with diphenylacetylene to afford azametallacyclobutene complex **6c** was fast, the relative rate constant for this process was kinetically inaccessible in all the successful runs of the study. The experimentally derived value of the rate constant k_5 for the unimolecular cycloreversion of **8b** at 5.0 ± 0.1 °C is (2.00 ± 0.02) × $10^{-3}\ s^{-1}$.

Insertion Reactions of Diazametallacycle Complexes 9a,b with Diphenylacetylene. Unlike the exchange reactions between zirconacycle compounds **4** and **8** with alkynes to generate azametallacyclobutene complexes **6** and symmetrical carbodiimides, a different type of reactivity was observed for diazametallacycle complexes **9a**,**b** when they were treated with 1 equiv of diphenylacetylene (**5a**). Zirconium diazacyclobutane species **9a**,**b** gave overall insertion products **10a**,**b** upon heating in the presence of diphenylacetylene (Scheme 5). Outlined in Scheme 7 are two possible mechanistic routes that lead to the generation of the six-membered zirconacycle complexes **10**. In the first pathway (a), direct insertion of diphenylacetylene into the nitrogen−carbon bond of diazametallacycle complex **9** occurs. To our knowledge, a direct insertion of this type is unprecedented.

The second proposed pathway (b) takes place by initial cycloreversion of diazametallacycle complex **9** to generate the transient zirconocene imido species **7c** and the organic carbodiimide RN═C═NR. Once the coordinatively unsaturated 16-electron imidozirconocene complex **7c** has formed, it can be trapped by an overall [2 + 2] cycloaddition reaction with free carbodiimide to

regenerate the starting material or by alkyne **5a** to form the corresponding diazametallacyclobutene complex **6**. The final six-membered zirconacycle complex **10** is then formed by direct insertion of the N−C double bond in free carbodiimide **3** into the zirconium−carbon bond of **6**.

We favor pathway (b) for two reasons. First, carbodiimide insertion into a metal−carbon bond is well precedented.[31−33] For example, Gamboratta and co-workers report the insertion of (*p*-Tol)N=C=N(*p*-Tol) into the zirconium−carbon σ bond of dimethylzirconocene.[34,35] Second, **10a**−**c** can be prepared independently by treatment of azametallacyclobutene complex **6e** with carbodiimides RN=C=NR (R = Cyc, *i*-Pr, *p*-Tol) at 25 °C (Scheme 5). This reaction is very rapid compared to the reaction of carbodiimide adduct **9** with diphenylacetylene (**5a**), supporting the conclusion that **6e** is a kinetically competent intermediate for the conversion of **9** to **10**. The rapid rate of reaction of **6e** with (*i*-Pr)N=C=N(*i*-Pr) (**3c**) is consistent with our kinetic study establishing an associative pathway that is second order overall, first order in [**6e**] and first order in [**3c**], for this reaction.

Insertion Reactions of Diazametallacyclobutene Complexes 6a,c with (*p*-Tol)N=C=N(*p*-Tol) (3e). To better understand the nature of the direct insertion of free carbodiimide into the zirconium−carbon bond of azametallacyclobutene complexes, we treated **6a** with (*p*-Tol)N=C=N(*p*-Tol) in the presence of $Me_3SiN{=}C{=}NSiMe_3$. The six-membered zirconacycle **11** was formed in high yield (eq 11). We propose a direct carbodiimide insertion that is analogous to the mechanism established for the reaction between azametallacyclobutene complex **6e** and (*i*-Pr)N=C=N(*i*-Pr) (**3c**) to generate **10b** (Scheme 7). The fact that there is no observable insertion of free $Me_3SiN{=}C{=}NSiMe_3$ into the zirconium−carbon bond of **6a** under the reaction conditions employed suggests that there is a strong steric effect in the insertion reaction. When aryl analogue **6c** was treated with (*p*-Tol)N=C=N(*p*-Tol) in the presence of either $Me_3SiN{=}C{=}NSiMe_3$ or (*t*-Bu)N=C=N(*t*-Bu), complex **12** was the only product (eq 11). These results further support the steric control hypothesis.

Exchange Reactions of Diazametallacycle Complex 4a with Symmetrical Carbodiimides. The stoichiometric exchange between diazametallacycle complex **4a** and carbodiimides to afford a new zirconacycle with the release of carbodiimide **3a** is directly analogous to the mechanistic pathway that Weiss and co-workers postulated for tungsten imido-catalyzed metathesis reactions between carbodiimides (Scheme 1). We saw the opportunity to utilize the zirconium diazametallacycle complexes in the exchange reaction with other carbodiimides as a model system to gain mechanistic insight into this type of reaction.

There are two reasonable mechanistic pathways for this process. One, depicted in Scheme 8, involves an

Scheme 8

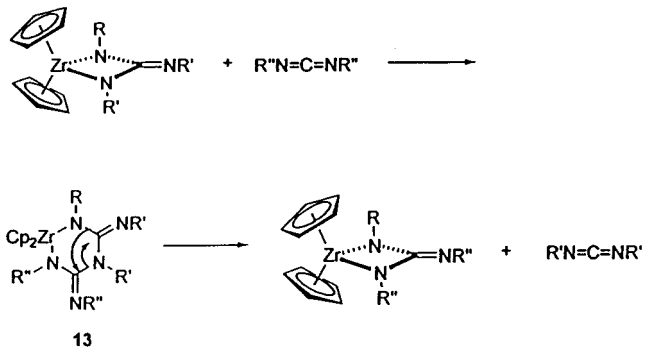

associative pathway in which the reactant carbodiimide directly inserts into the zirconium−nitrogen bond of the four-membered ring to generate six-membered zirconacycle **13**. Extrusion of the symmetrical carbodiimide **3a** from **13** would give the new metallacyclobutane complex. The second proposed pathway is a dissociative process (Scheme 6), analogous to the mechanism established for the exchange reaction of **4a** with diphenylacetylene (Scheme 2).

To distinguish these possibilities, kinetic analysis of the carbodiimide exchange reaction was carried out under pseudo-first-order conditions. Because of the limited solubility of 1,3-di-*p*-tolylcarbodiimide (**3e**) under the reaction conditions, the study was carried out with excess concentrations of **4a** and **3a**, with carbodiimide **3e** as limiting reactant. The reaction was found to be first order in **3e**, and the experimental data are consistent with the derived rate law in eqs 13−15. The rate constant ratio of $k_1k_{10}/k_2 = (8.1 \pm 0.1) \times 10^3\ s^{-1}$ was obtained from the plot of $1/k_{obs}$ vs [**3a**]/[**4a**] (Figure 6). The kinetic data support the dissociative process outlined in Scheme 6.

Because we could not reach saturation conditions in [**4a**], we were unable to directly obtain the value for the rate constant k_1. To address this problem, we initiated a kinetic analysis of a related system in which the reactant carbodiimide (**3e**) was replaced with 1,3-di-*m*-tolylcarbodiimide (**3f**) to overcome the solubility problems that we encountered with high concentrations of **3e**. Pseudo-first-order conditions were maintained during the course of the reaction by using excess concentrations of meta-substituted aryl carbodiimide **3f** and silyl-substituted carbodiimide **3a**. Saturation kinetics were observed at high concentrations of **3f** and the value for k_1 could be obtained ($(4.82 \pm 0.02) \times 10^4\ s^{-1}$). Additionally, the ratio k_2/k_{11} equals 0.8. Thus, trapping of imidozirconocene **7a** with silyl-substituted carbodiimide **3a** occurs 1.25 times faster than the rate of trapping **7a** with **3f**.

Since k_1 corresponds to the rate constant for the unimolecular formal [2 + 2] retrocycloaddition of zirconacycle **4a** to generate zirconocene imido complex **7a** and carbodiimide **3a**, the value experimentally derived for k_1 in the exchange reaction of **4a** with **3f** should be the same as that determined in the exchange reaction between **4a** and the para-substituted carbodiimide **3e**. Substituting the experimentally determined k_1 value obtained in the exchange reaction between **4a** and **3f** ($(4.82 \pm 0.02) \times 10^{-4}\ s^{-1}$) into the experimentally derived rate constant ratio of $k_1k_{10}/k_2 = (8.1 \pm 0.1) \times$

(31) Li, M.-D.; Chang, C. C.; Wang, Y.; Lee, G. H. *Organometallics* **1996**, *15*, 2571.
(32) Chang, C. C.; Hsiung, C.-S.; Su, H.-L.; Srinivas, B.; Chiang, M. Y.; Lee, G.-H.; Wang, Y. *Organometallics* **1998**, *17*, 1595.
(33) Shapiro, P. J.; Henling, L. M.; Marsh, R. E.; Bercaw, J. E. *Inorg. Chem.* **1990**, *29*, 4560.
(34) Gambarotta, S. S.; Floriani, C.; Chiesi-Villa, A.; Guastini, C. *Inorg. Chem* **1985**, *24*, 654.
(35) Gambarotta, S. S.; Floriani, C.; Chiesi-Villa, A.; Guastini, C. *J. Am. Chem. Soc.* **1985**, *107*, 6278.

10^3 s^{-1} measured in the reaction between **4a** and **3e**, we calculate $k_{10}/k_2 = 1.67$. Thus, for this case, the trapping of imidozirconocene **7a** with para-substituted aryl carbodiimide **3e** is over 1.5 times faster than the rate of trapping **7a** with **3a**. We attribute the difference in trapping rates of imidozirconocene complex **7a** with **3e**,**f** to steric factors in the aryl carbodiimides.

Qualitatively, the relative rates of reaction with carbodiimides were much faster for this aryl imido species $Cp_2Zr{=}N$-2,6-Me_2Ph than the N-alkylated imido complex $Cp_2Zr{=}N$-*t*-Bu. Since we know the k_1 value for the formal [2 + 2] retrocycloaddition reaction of **8a** to generate **7b** and alkyne **3a** is an order of magnitude greater than in the case of the N-*t*-Bu analogue **4a**, we can infer that zirconocene imido **7b** is being generated in the carbodiimide exchange reactions in an analogous dissociative mechanism that has been established with **4a** and carbodiimides **3e**,**f**.

Imido Group Transfer. Our experimental results suggest that arylzirconocene imido complexes are thermodynamically favored over the corresponding N-alkyl complexes. In all the cases examined in this study, retrocycloaddition of diazametallacycle complexes **8** (Scheme 4) and **9** (Scheme 7) resulted in the generation of zirconocene arylimido complexes **7b**,**c**, respectively, with release of symmetrical dialkylcarbodiimides. The thermodynamic driving force could be due to either the inherent stability of the arylimido complex, the stability of the symmetrical carbodiimide, or both. However, when diazametallacycle **8a** was treated with an equimolar amount of $Cp_2(THF)Zr{=}N$(*t*-Bu) (**2a**), quantitative conversion to the zirconocene imido complex $Cp_2(THF)Zr{=}N$(2,6-Me_2Ph) (**2b**) and diazametallacycle complex **4a** was observed (eq 17). This result is consistent with the postulate of greater thermodynamic stability of the N-aryl imidozirconocene complexes over their N-alkyl analogues.

During the course of this study, cycloreversion of **4a** consistently resulted in the generation of $Cp_2Zr{=}N$(*t*-Bu) (**7a**) and the release of $Me_3SiN{=}C{=}NSiMe_3$. However, from previous studies,[26] treatment of diazametallacycle complex **4b** with 1 equiv of (*i*-Pr)N=C=N(*i*-Pr) resulted in generation of the symmetrical metallacycle **14** with the release of (*t*-Bu)N=C=N(*i*-Pr) (Scheme 9). The proposed mechanism for this process invokes initial cycloreversion of **4b** to generate the zirconocene imido complex **7d** and the unsymmetrical carbodiimide. Once complex **7d** forms, it is rapidly trapped by (*i*-Pr)N=C=N(*i*-Pr) to generate **14**. In contrast to this observation, we have never observed the release of an aryl/alkyl carbodiimide from an appropriately substituted diazametallacycle.

Scheme 9

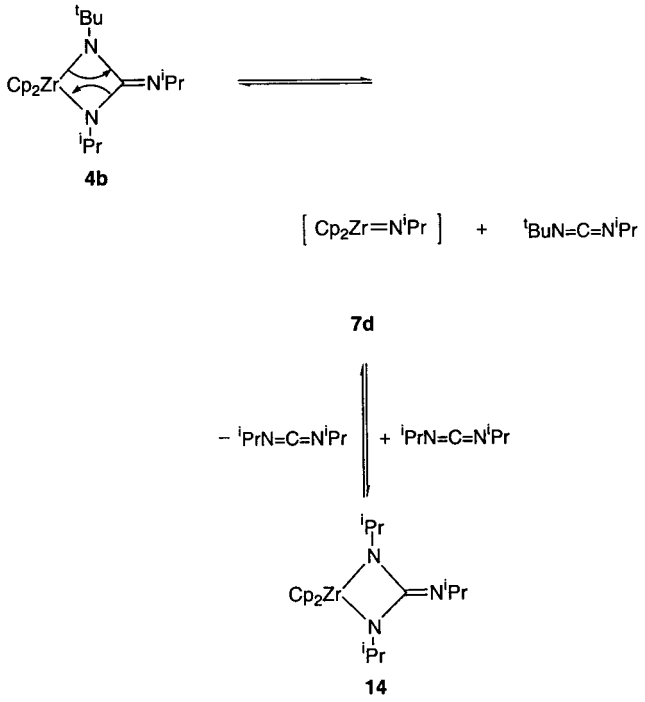

Conclusions

In this study, we have established that the overall [2 + 2] cycloadditions that take place between imidozirconocene complexes and heterocumulenes are reversible and that this reversibility is general. Thus, the system allows zirconocene complexes to mediate overall heterocumulene metathesis reactions. These reactions provide a useful method for the generation of new zirconium-containing metallacycles and small, unsaturated organic substrates. The detailed mechanistic study reported in this paper has allowed us to define the following properties of this system.

1. Kinetic studies have established that the heterocumulene exchange takes place by a dissociative pathway that involves initial cleavage of the four-membered metallacycle and regeneration of the transient 16-electron imidozirconocene intermediate $Cp_2Zr{=}NR$.

2. The overall course and rate of these reactions are quite sensitive to the presence of other unsaturated molecules and to the structural and electronic properties of both the metallacycle and heterocumulene substrates. For example, when a zirconocene/heterocumulene adduct metallacycle is thermally cleaved in the presence of an alkyne, the 16-electron zirconocene imido complex so generated is trapped by the alkyne to afford the corresponding azametallacyclobutene complex. The activation barrier for the initial metallacycle cleavage step in the retrocycloaddition is lower when it is possible to generate an imido complex with an aryl rather than an alkyl N substituent (e.g., the cleavage of N-aryl metallacycle **8a** occurs more rapidly than the cleavage of N-alkyl-substituted metallacycle **4a**). In general, we find that *N*-arylimidozirconocene complexes form preferentially over *N*-alkylimido complexes.

3. The metallacyclobutenes undergo further insertion reactions with carbodiimides, leading to ring-expanded six-membered heterometallacycles (e.g., **10a**−**c**). This requires relatively small N substitutents; when the carbodiimide is sterically bulky, this reaction does not occur.

4. The cycloaddition/ring expansion process can also be carried out in the reverse sequence: that is, by preparing the heterocumulene adduct first and then treating it with an alkyne. Interestingly, this results in formation of the *same* six-membered metallacycle (e.g. **10a**,**b)** as that formed when the metallacyclobutene is treated with a carbodiimide. This implicates the metallacyclobutene (e.g., **6e**, Scheme 7) as an intermediate in both of these reactions.

5. Kinetic studies on the reaction of zirconacyclobutene **6e** with (*i*-Pr)N=C=N(*i*-Pr) to generate **10b**

support an associative pathway for the insertion of (*i*-Pr)N═C═N(*i*-Pr) into the zirconium−carbon bond of **6e**.

Experimental Section

General Methods. Unless otherwise noted, all manipulations were carried out under an inert atmosphere in a Vacuum Atmospheres 553-2 drybox with an attached M6-40-Dritrain or with use of standard Schlenk or vacuum line techniques. Degassed solutions were frozen to −196 °C, evacuated under high vacuum, and thawed.

Sealed NMR tubes (Wilmad 505-PP and 504-PP) were prepared by attaching Cajon adapters directly to Kontes vacuum stopcocks and flame-sealing. J. Young tubes refer to resealable NMR tubes fitted with Teflon stopcocks. Glassware was dried in an oven at 150 °C before use. Pentane, hexanes, diethyl ether, toluene, benzene, and THF were distilled from Na/benzophenone. Sieves (4 Å) were activated by heating under vacuum at 200 °C for 24 h. The reagents 2,6-dimethylaniline and 2,6-diisopropylaniline were purchased from Aldrich, distilled from CaH_2, and stored over 4 Å sieves in the glovebox. Diphenylacetylene was purchased from Aldrich and sublimed prior to use. Carbodiimides **3a**−**e** were purchased from Aldrich and used without further purification. Complexes **2a**−**c**,[25a,26] **3f**,[25b] **4a**−**d**,[26] **6a**−**d**,[9,10,25] **8a**−**e**,[26] and **9a**,**b**[26] were prepared by literature methods and crystallized prior to use.

All ^{1}H and ^{13}C{^{1}H} NMR spectra were recorded on commercial Bruker AMX 300 and DRX 500 spectrometers. Chemical shifts (δ) are reported in parts per million (ppm) relative to residual protiated solvent: C_6D_6 (7.15 ppm), THF-d_8 (3.58 ppm). All ^{13}C{^{1}H} NMR spectra were recorded at 100 MHz and are reported in ppm relative to the carbon resonance of the deuterated solvent C_6D_6 (128.0 ppm). Mass spectrometric analyses were obtained at the University of California, Berkeley Mass Spectrometry Facility, on a VT Prospec mass spectrometer. Elemental analyses were performed at the University of California, Berkeley Microanalytical Facility, on a Perkin-Elmer 2400 Series II CHNO/S analyzer. Kinetic studies were performed with a Hewlett-Packard 8453 UV−vis spectrometer.

$Cp_2Zr(N(t\text{-}Bu)C{=}N(m\text{-}Tol)N(m\text{-}Tol))$ (4e). A glass reaction vessel equipped with a Teflon stopcock was charged with $Cp_2(THF)Zr{=}N\text{-}t\text{-}Bu$ (**2a**; 257 mg, 0.70 mmol) and C_6H_6 (10 mL). The solution was stirred, and 1,3-di-*m*-tolylcarbodiimide (156 mg, 0.70 mmol) was added dropwise. The solution turned from yellow to purple immediately. After the mixture was stirred at 25 °C for 20 min, the solvent was removed under reduced pressure to afford a purple solid. The solid was crystallized from benzene layered with hexanes at 25 °C for 2 days to afford deep purple needles (259 mg, 72% yield). ^{1}H NMR (C_6D_6): δ 7.02 (t, J = 7 Hz, 1H, aryl), 6.91 (m, 3H, aryl), 6.52 (s, 1H, aryl), 6.50 (d, J = 7 Hz, 1H, aryl), 6.45 (d, J = 7 Hz, 1H, aryl), 5.99 (s, 10OH, C_5H_5), 2.21 (s, 3H, CH_3), 2.09 (s, 3H, CH_3), 1.48 (s, 9H, $C(CH_3)_3$); ^{13}C{^{1}H} NMR (C_6D_6): δ 151.2, 150.2, 142.8, 137.4, 136.9, 128.3, 123.9, 121.9, 120.6, 119.9, 119.8, 117.9, 115.8, 108.8, 34.4, 30.2, 25.8, 21.8, 21.6. Anal. Calcd for $C_{29}H_{33}N_3Zr$: C, 67.66; H, 6.46; N, 8.16. Found: C, 67.99; H, 6.64; N, 7.86.

$Cp_2Zr(N(2,6\text{-}i\text{-}Pr_2Ph)C(Ph){=}C(Ph))$ (6e). The zirconocene imido complex **2c** (380 mg, 0.81 mmol) and diphenylacetylene (145 mg, 0.81 mmol) were dissolved in 5 mL of benzene. A forest green color developed immediately. After it was stirred for 3 h at 25 °C, the reaction mixture was evaporated to dryness, and the resulting green solid was triturated with Et_2O (2 × 3 mL). The last traces of solvent were removed at reduced pressure to obtain analytically pure **6e** as a dark green powder (359 mg, 77% yield). ^{1}H NMR (C_6D_6): δ 7.02 (t, J = 15 Hz, 2H, aryl), 7.19 (m, 3H, aryl), 7.01 (m, 4H, aryl), 6.95 (d, J = 7 Hz, 2H, aryl), 6.92 (d, J = 7 Hz, 2H, aryl), 5.8 (s, 10H, C_5H_5), 3.46 (m, 2H, $CH(CH_3)_2$), 1.21 (d, J = 6 Hz, 6H, $CH(CH_3)_2$), 0.93 (d, J = 6 Hz, 6H, $CH(CH_3)_2$); ^{13}C{^{1}H}NMR (C_6D_6): δ 181.8, 149.2, 147.1, 141.1, 131.9, 131.8, 130.5, 127.1, 127.0, 124.1, 123.4, 122.4, 111.0. Anal. Calcd for $C_{36}H_{37}NZr$: C, 75.21; H, 6.49; N, 2.44. Found: C, 75.40; H, 6.68; N, 2.26.

10a. Method A. Diphenylacetylene (55 mg, 0.30 mmol) and diazametallacycle **9a** (184 mg, 0.30 mmol) in benzene (5 mL) were added to a glass reaction vessel that was equipped with a Teflon stopcock and stir bar. The solution was heated to 75 °C, and an orange color developed slowly. After it was heated for 15 h, the solvent was removed at reduced pressure to leave an orange solid which was dissolved in hexanes (3 mL) and stored at −35 °C for 45 days to afford orange prisms (152 mg, 65% yield). ^{1}H NMR (C_6D_6): δ 7.22 (d, J = 5 Hz, 2H, aryl), 6.85 (t, J = 15 Hz, aryl), 6.72 (m, 5H, aryl), 6.42 (d, J = 7 Hz, 2H, aryl), 6.36 (s, 5H, C_5H_5), 5.95 (s, 5H, C_5H_5), 3.72 (m, 2H, $CH(CH_3)_2$), 3.36 (m, 1H, CH), 3.15 (m, 1H, CH), 2.38−0.68 (m, 20H, cyclohexyl CH_2's), 1.61 (d, J = 6 Hz, 3H, $CH(CH_3)_2$), 1.53 (d, J = 7 Hz, 3H, $CH(CH_3)_2$), 1.00 (d, J = 7 Hz, 3H, $CH(CH_3)_2$), −0.03 (d, J = 7 Hz, 3H, $CH(CH_3)_2$). ^{13}C{^{1}H} NMR (C_6D_6): δ 155.5, 150.9, 145.9, 144.2, 139.3, 131.92, 130.4, 130.2, 129.6, 128.5. 127.2, 126.6, 126.2, 125.6, 124.9, 124.2, 113.5, 111.2, 66.2, 56.3, 37.9, 35.3, 33.2, 29.2, 28.2, 28.1, 27.3, 27.1, 26.9, 26.3, 25.8, 25.5, 25.1, 24.5, 23.1. HREIMS: m/z calcd for $C_{49}H_{59}N_3Zr$ 779.3760, found 779.3756.

Method B. Diazametallacyclobutene **6e** (100 mg, 0.17 mmol) and 1,3- dicyclohexylcarbodiimide (36 mg, 0.17 mmol) were dissolved in benzene (3 mL). An orange color developed over 30 min. The solution was stirred for 1 h at 25 °C and evaporated to dryness at reduced pressure to afford an orange powder. The solid was redissolved in Et_2O (2 mL), and the resulting solution was stored at −35 °C for 2 days. Complex **10a** was isolated as orange crystals (99 mg, 75% yield) of **10a**.

10b. Method A. Diphenylacetylene (58 mg, 0.326 mmol) and diazametallacycle **9b** (170 mg, 0.326 mmol) in benzene (5 mL) were added to a glass reaction vessel that was equipped with a Teflon stopcock and stir bar. The solution was heated to 75 °C, and a yellow color developed after heating for 20 h. The solvent was removed at reduced pressure to leave a yellow oil which was dissolved in Et_2O (2 mL) and stored at −35 °C for 2 days to afford analytically pure **10b** as a yellow powder (162 mg, 71%). ^{1}H NMR (C_6D_6): δ 7.50 (t, J = 6 Hz, 1H, aryl), 7.17−6.45 (13H, aryl), 6.34 (s, 5H, C_5H_5), 5.92 (s, 5H, C_5H_5), 3.69 (m, 1H, $CH(CH_3)_2$), 2.89 (m, 1H, $CH(CH_3)_2$), 2.68 (m, 1H, $CH(CH_3)_2$), 1.95 (d, J = 5 Hz, 3H, $CH(CH_3)_2$), 1.77 (d, J = 5 Hz, 3H, $CH(CH_3)_2$), 1.60 (d, J = 5 Hz, 3H, $CH(CH_3)_2$), 1.52 (d, J = 5 Hz, 3H, $CH(CH_3)_2$), 1.30 (d, J = 5 Hz, 3H, $CH(CH_3)_2$), 1.00 (d, J = 5 Hz, 3H, $CH(CH_3)_2$), 0.27 (d, J = 5 Hz, 3H, $CH(CH_3)_2$), −0.03 (d, J = 5 Hz, 3H, $CH(CH_3)_2$). ^{13}C{^{1}H} NMR (C_6D_6): δ 154.9, 150.8, 145.8, 144.6, 144.2, 143.9, 139.3, 131.9, 130.2, 130.1, 129.5, 128.6, 128.5, 128.4, 127.8, 127.4, 127.2, 126.7, 126.2, 125.7, 124.9, 124.2, 113.6, 113.5, 111.3, 111.2, 55.2, 48.0, 28.2, 27.4, 27.0, 26.4, 25.0, 24.8, 24.7, 24.4, 23.2, 22.4, 19.5. HREIMS: m/z calcd for $C_{43}H_{51}N_3Zr$ 701.3140, found 701.3133.

Method B. Diazametallacyclobutene **6e** (81 mg, 0.14 mmol) and 1,3- diisopropylcarbodiimide (28 mg, 0.14 mmol) were dissolved in 3 mL of benzene. The color changed from green to yellow while the solution was stirred at 25 °C for 1 h. The solvent was removed at reduced pressure and redissolved in Et_2O (2 mL). The solution was stored at −35 °C for 2 days. A yellow powder (80 mg, 82% yield) of **10b** was obtained.

10c. 1,3-Di-*p*-tolylcarbodiimide (46 mg, 0.21 mmol) and metallacyclobutene complex **6e** (70 mg, 0.21 mmol) were dissolved in benzene (5 mL). The solution turned from green to orange while it was stirred at 25 °C for 1 h. The reaction mixture was evaporated to dryness, the residue was redissolved in Et_2O (3 mL), and this solution was stored at −35 °C for 1 day. Analytically pure **10c** was obtained as an orange powder (101 mg, 73% yield). ^{1}H NMR (C_6D_6): δ 7.28 (d, J = 5 Hz, 2H, aryl), 7.09 (m, 6H, aryl), 6.86 (d, J = 5 Hz, 2H, aryl), 6.70 (m, 11H, aryl), 6.43 (s, 5H, C_5H_5), 5.59 (s, 5H, C_5H_5), 4.24 (m, 1H, $CH(CH_3)_2$), 2.65 (m; 1H, $CH(CH_3)_2$), 2.17 (s, 3H, CH_3),

2.04 (s, 3H, CH_3), 1.88 (d, J = 5 Hz, 3H, CH(CH_3)$_2$), 1.65 (d, J = 5 Hz, 3H, CH(CH_3)$_2$), 0.95 (d, J = 5 Hz, 3H, CH(CH_3)$_2$), −0.05 (d, J = 10 Hz, 3H, CH(CH_3)$_2$). ^{13}C{^{1}H} NMR (C_6D_6): δ 159.1, 146.7, 146.1, 145.6, 145.6, 144.0, 139.9, 129.0, 128.5, 128.5, 127.4, 127.1, 126.7, 126.5, 125.0, 124.8, 124.4, 121.2, 114.8, 111.6, 65.8, 27.6, 27.6, 27.5, 25.7, 24.6, 23.3, 21,0. 21.0, 20.8, 15.5. Anal. Calcd for $C_{51}H_{51}N_3Zr$: C, 76.84; H, 6.45; N, 5.27. Found: C, 76.45; H, 6.68; N, 5.03.

11. Metallacyclobutene complex **6a** (70 mg, 0.21 mmol) and 1,3-di-*p*- tolylcarbodiimide (45 mg, 0.20 mmol) were dissolved in benzene (5 mL). The solution turned from green to orange while it was stirred at 25 °C for 1 h. After it was stirred overnight at 25 °C, the reaction mixture was evaporated to dryness to afford an orange solid. This solid was dissolved in hexanes (3 mL) and stored at −35 °C for 7 days. Analytically pure **11** was obtained as an orange powder (137 mg, 97% yield). ^{1}H NMR (C_6D_6): δ 7.62 (d, J = 7 Hz, 2H, aryl), 7.51 (d, J = 7 Hz, 1H, aryl), 7.05 (m, 10H, aryl), 6.98 (m, 5H, aryl), 6.20 (s, 5H, C_5H_5), 5.54 (s, 5H, C_5H_5), 2.14 (s, 3H, CH_3), 2.14 (s, 3H, CH_3), 0.67 (s, 9H, C(CH_3)$_3$). ^{13}C{^{1}H} NMR (C_6D_6): δ 150.3, 147.1, 141.5, 140.4, 133.3, 131.9, 131.6, 130.2, 129.4, 128.9, 128.6, 128.5, 128.5, 127.5, 127.2, 126.6, 123.8, 122.2, 112.8, 110.1, 89.6, 21.9, 21.8, 11.9, 5.7. HREIMS: *m*/*z* calcd for $C_{43}H_{43}N_3Zr$ 692.2564. found 692.2582.

12. A J. Young NMR tube was charged with Cp_2Zr(N(2,6-$Me_2C_6H_3$)C═N($SiMe_3$)N($SiMe_3$)) (**8a**; 10.0 mg, 0.02 mmol), 1,4-dimethoxybenzene (5.2 mg, 0.038 mmol), diphenylacetylene (5.0 mg, 0.028 mmol), and 0.6 mL of C_6D_6. A green color developed immediately. A single-pulse ^{1}H NMR spectrum was acquired in which the resonances of the cyclopentadienyl ligands of **6c** were integrated against the methoxy groups of 1,4-dimethoxybenzene. 1,3-Di-*p*-tolylcarbodiimide (6.2 mg, 0.028 mmol) was added to the reaction mixture. After 1 h, another ^{1}H NMR spectrum was measured as described above; a 90% yield of six-membered zirconacycle **12** was obtained. Complex **12** was only characterized by ^{1}H NMR spectroscopy and MS analysis since its analogue, zirconacycle complex **11**, was fully characterized. ^{1}H NMR (C_6D_6): δ 7.55 (d, J = 7 Hz, 2H, aryl), 7.1 (m, 7H, aryl), 6.95 (m, 12H, aryl), 6.44 (s, 5H, C_5H_5), 5.47 (s, 5H, C_5H_5), 2.26 (s, 3H, CH_3), 2.11 (s, 3H, CH_3), 2.05 (s, 6H, CH_3). MS (EI): *m*/*z* calcd 739, found 739.

Reactions of Diazametallacycle Complexes 4a, 8a, and 8b with Alkynes. In a typical reaction, a J. Young NMR tube was charged with Cp_2Zr(N(2,6-$Me_2C_6H_3$)C═N(*t*-Bu)N(*t*-Bu)) (**8b**; 10.0 mg, 0.02 mmol), 1,4-dimethoxybenzene (5.5 mg, 0.04 mmol), and 0.6 mL of C_6D_6. A single-pulse ^{1}H NMR spectrum was acquired in which the resonances of the cyclopentadienyl ligands of **8b** were integrated against the methoxy groups of 1,4-dimethoxybenzene. Diphenylacetylene (5.0 mg, 0.03 mmol) was added to the NMR tube at 25 °C in the glovebox, and the solution turned from purple to green within seconds after the addition. After 20 min, another ^{1}H NMR spectrum was obtained as described above; a 97% yield of azametallacyclobutene **6c** was measured. ^{1}H NMR spectrometry indicated that 1,3-di-*tert*-butylcarbodiimide (δ 1.16 in C_6D_6) was formed in 91% yield. The ^{1}H NMR spectrum of 1,3-di-*tert*-butylcarbodiimide was identical with that of an authentic sample purchased from Aldrich. The ^{1}H NMR spectrum for **6c** was compared with literature values.[9] ^{1}H NMR (THF-d_8): δ 7.3 (t, 2H, aryl), 6.91 (m, 6H, aryl), 6.75 (m, 4H, aryl), 6.51 (t, 1H, aryl), 6.12 (s, 10H, C_5H_5), 2.16 (s, 6H, CH_3).

Reactions of 4a and 8a with Symmetrical Carbodiimides. The general procedure used was identical with that described above for the reaction of **8b** with diphenylacetylene (**5a**). In a typical reaction, a J. Young NMR tube was charged with Cp_2Zr(N(2,6-$Me_2C_6H_3$)C═N($SiMe_3$)N($SiMe_3$)) (**8a**; 10.0 mg, 0.02 mmol), 1,4-dimethoxybenzene (9.6 mg, 0.07 mmol), and 0.6 mL of C_6D_6. 1,3-Diisopropylcarbodiimide (3.5 mg, 4.4 μL, 0.03 mmol) was added to the NMR tube. The reaction mixture turned purple immediately. It was determined that Cp_2Zr(N(2,6-$Me_2C_6H_3$)C═N(*i*-Pr)N(*i*-Pr)) (**8c**) and 1,3-bis(trimethylsilyl)carbodiimide were formed in 97% and 100% yields, respectively, by integration against the internal standard 1,4-dimethoxybenzene. Complex **8c** was identified by comparison of its NMR spectrum with those in the literature.[26] ^{1}H NMR (C_6D_6): δ 7.18 (d, J = 7 Hz, 2H, aryl), 6.96 (t, J = 15 Hz, IH, aryl), 5.80 (s, 10H, C_5H_5), 4.01 (m, 2H, CH(CH_3)$_2$), 2.21 (s, 6H, aryl CH_3's), 1.32 (d, J = 6 Hz, 6H, CH(CH_3)$_2$), 1.18 (d, J = 6 Hz, 6H, CH(CH_3)$_2$).

Kinetic Studies of the Reaction between 4a and Diphenylacetylene (5a). UV−vis spectrometry was used to study the exchange reaction between diazametallacycle complex **4a** and diphenylacetylene (**5a**) to generate azametallacyclobutene **6a** and 1,3-bis(trimethylsilyl)carbodiimide (**3a**). A stock solution of **4a** (7.5×10^{-4} M) was prepared by weighing 44.7 mg (0.094 mmol) into a 25.00 ± 0.01 mL volumetric flask. Dimethylzirconocene (12.6 mg, 0.05 mmol) was added, and the mixture was diluted to the final volume with benzene to give a concentration of 3.75×10^{-3} M for **4a**. The solution was mixed well, and 1 mL was transferred with a volumetric pipet to a second 5.00 ± 0.01 mL volumetric flask, followed by dilution to the final volume with benzene. The 7.5×10^{-4} M solution of **4a** was stored in the drybox at −35 °C. A typical 3.75×10^{-2} M stock solution of **5a** was prepared by weighing diphenylacetylene (66.8 mg, 0.38 mmol) into a 10 mL volumetric flask and diluting to the final volume with benzene. A stock solution of 1,3-bis(trimethylsilyl)carbodiimide (**3a**; 7.5×10^{-2} M) was prepared by weighing 69.9 mg (0.375 mmol) of **3a** into a 10.00 ± 0.01 mL volumetric flask and diluting to the final volume with benzene. A serial dilution to afford a 7.5×10^{-2} M stock solution of **3a** was done by transferring 1 mL of a 3.75×10^{-2} M solution of **3a** with a volumetric pipet into a 5 mL volumetric flask and diluting to the final volume with benzene. Both stock solutions of **3a** and **5a** were stored in the drybox at −35 °C.

In a typical kinetic run, stock solutions of **4a**, **3a**, and **5a** were allowed to thaw in the drybox and 1 mL from a 7.5×10^{-4} M stock solution of **4a**, 1 mL from a 3.75×10^{-2} M stock solution of **5a**, and 1 mL of 7.5×10^{-2} M **3a** were transferred with volumetric pipets to a 1 mm gastight cuvette. The final concentrations were 2.50×10^{-4} M for **4a**, 1.25×10^{-2} M for **5a**, and 2.50×10^{-3} for **3a**. The cuvette was equipped with a Kontes Teflon stopcock and placed in the temperature control unit of the UV−vis spectrometer. Data were collected at 95 s time intervals for over 8 half-lives at 15.4 ± 0.1 °C. The absorbance of reactant azametallacyclobutene **6a** (λ = 420 nm) was plotted vs time, and the data were analyzed with an exponential fitting program.

Kinetic Studies of the Reaction between 8a and Diphenylacetylene (5a). UV−vis spectrometry was used to study the exchange reaction between diazametallacycle complex **8a** and diphenylacetylene to generate azametallacyclobutene **6c** and carbodiimide **3a**. A typical 0.002 M stock solution of metallacycle **8a** was prepared by weighing 24.7 mg (0.05 mmol) **8a** into a 5.00 ± 0.01 mL volumetric flask. Dimethylzirconocene (9.5 mg, 0.04 mmol) was added, and the mixture was diluted to the final volume with benzene. The solution was mixed well, and 1 mL was transferred with a volumetric pipet to a second 5.00 ± 0.01 mL volumetric flask followed by dilution to the final volume with benzene. The 0.002 M solution of **8a** was stored in the drybox at −35 °C. A typical (0.05 M) stock solution of **5a** was prepared by weighing diphenylacetylene (44.6 mg, 0.25 mmol) into a 5 mL volumetric flask and diluted to the final volume with benzene. A serial dilution to afford a 0.01 M stock solution of **5a** was done by transferring 1 mL of a 0.05 M solution with a volumetric pipet into a 5 mL volumetric flask and diluting to the final volume with benzene. A similar procedure was used for the generation of a 0.05 M stock solution of carbodiimide **3a**. 1,3-Bis(trimethylsilyl)carbodiimide was weighed into a 5.00 ± 0.01 mL volumetric flask (46.6 mg, 0.25 mmol) and diluted to the

final volume with benzene. Both stock solutions of **3a** and **5a** were stored in the drybox at −35 °C.

In a typical kinetic run, stock solutions of **8a**, **5a**, and **3a** were allowed to thaw in the drybox, and 0.5 mL from a 0.002 M stock solution of **8a** and 1 mL of 0.05 M **3a** were transferred with volumetric pipets to a 1 mm gastight cuvette with a sidearm. The cuvette was equipped with a Kontes Teflon stopcock. An additional 0.5 mL of benzene was added via volumetric pipet. The stopcock was sealed to the UV−vis cell, and 1.0 mL of 0.01 M solution of **5a** was transferred to the sidearm of the cell. A rubber septum was wired onto the orifice of the sidearm to prevent the introduction of any adventitious oxygen or water into the system. The cuvette was removed from the drybox, and the solution was cooled to 5.0 ± 0.1 °C in the temperature control unit of the UV−vis spectrometer. Once the solution in the cuvette was cooled, the stopcock was adjusted to allow the flow of diphenylacetylene (**5a**) solution into the cell. The stopcock was tightly closed, and the cuvette was shaken to ensure a homogeneous solution. Data acquisition began after the solution was allowed to equilibrate to the bath temperature (ca. 60 s), and spectra were recorded at regular intervals (10 s) for over 4 half-lives of the reaction. The absorbance of metallacyclobutene **6c** was monitored (λ = 550 nm) and plotted vs time. The data were analyzed with an exponential fitting program.

Kinetic Studies of the Reaction between 8b and Diphenylacetylene (5a). A procedure similar to that used for the kinetic analysis of the reaction between **8a** and **5a** was utilized in this kinetic study. Stock solutions with weighed amounts of **8b**, **3b**, and **5a** in benzene were prepared and stored at −35 °C in the drybox prior to individual kinetic runs. Data were collected at 10 s time intervals for over 4 half-lives, and the absorbance of product azametallacyclobutene **6c** was plotted vs time.

Kinetic Studies of the Reaction between Azametallacyclobutene Complex 6e and 1,3-Diisopropylcarbodiimide (3c). A procedure similar to that carried out for the kinetic analysis of the reaction between diazametallacycle complex **4a** and diphenylacetylene (**5a**) was utilized in this kinetic study. Stock solutions with weighed amounts of **6a** and **3c** in benzene were prepared and stored at −35 °C in the drybox prior to individual kinetic runs. Data were collected at 20 s time intervals for over 11 half-lives at 15.4 ± 0.1 °C. The absorbance of reactant azametallacyclobutene **6e** (λ 420 nm) was plotted vs time, and the data were analyzed with an exponential fitting program.

Kinetic Studies of the Reaction between 4a and 1,3-Di-*p*-tolylcarbodiimide (3e). A procedure similar to that carried out for the kinetic analysis of the reaction between diazametallacycle complex **4a** and diphenylacetylene (**5a**) was utilized in this kinetic study. This system was modified by using excess concentrations of **4a** and $Me_3SiN{=}C{=}NsiMe_3$ (**3a**) relative to the concentration of (*p*-Tol)N=C=N(*p*-Tol) (**3e**). Stock solutions with weighed amounts of **4a**, **3a**, and **3e** in benzene were prepared and stored at −35 °C in the drybox prior to individual kinetic runs. Data were collected at 60 s time intervals at 15.4 ± 0.1 °C for over 5 half-lives, and the absorbance of diazametallacycle complex **4e** was monitored (λ 420 nm) and was plotted vs time.

Kinetic Studies of the Reaction between 4a and 1,3-Di-*m*-tolylcarbodiimide (3f). A procedure similar to that used for the kinetic analysis of the reaction between diazametallacycle complex **4a** and (*p*-Tol)N=C=N(*p*-Tol) (**3e**) was utilized in this kinetic study. This system was modified by using excess concentrations of (*m*-Tol)N=C=N(*m*-Tol) (**3f**) and $Me_3SiN{=}C{=}NSiMe_3$ (**3a**) relative to the concentration of diazametallacycle complex **4a**. Stock solutions with weighed amounts of **4a**, **3a**, and **3e** in benzene were prepared and stored at −35 °C in the drybox prior to individual kinetic runs. Data were collected at 60 s time intervals at 15.4 ± 0.1 °C for over 5 half-lives, and the absorbance of diazametallacycle complex **4f** was monitored (λ 600 nm). The absorbance of **4f** was plotted vs time, and the data were analyzed with an exponential fitting program.

X-ray Structure Determination of 4a and 10a. Both crystals were mounted on quartz fibers using Paratone N hydrocarbon oil. For both compounds, measurements were made on a SMART CCD area detector with graphite-monochromated Mo Kα radiation. Data were integrated by the program SAINT. The data were corrected for Lorentz and polarization effects and analyzed for agreement and possible absorption using XPREP.[36] An empirical absorption correction based on comparison of redundant and equivalent reflections as applied using SADABS[37] (7d, $T_{min} = 0.91$, $T_{min} = 0.86$; 10a, $T_{min} = 0.897$, $T_{min} = 0.818$; 10b, $T_{min} = 0.97$, $T_{min} = 0.81$). The structures were solved by direct methods and expanded using Fourier techniques. The non-hydrogen atoms were refined anisotropically. Plots of $\sum w(|F_o| - |F_c|)^2$ vs $|F_o|$, the reflection order in data collection, $(\sin\theta)/\lambda$, and various classes of indices showed no unusual trends. All calculations were performed using the teXsan[38] crystallographic software package of Molecular Structure Corp.

For compound **4a**, all non-hydrogen atoms were refined anisotropically except for Si3 and C2. Hydrogen atoms were included but not refined. Disorder was found in the structure of the molecule between one $SiMe_3$ group and the ^{t}Bu group. A partially occupied silicon atom, Si3, was placed in a fixed idealized location along the N1−C2 bond axis 1.67 Å from N1. The population of the majority silicon, Si1, was allowed to vary, and the populations of Si3 and C2 were tied to that of Si1; the occupancy of Si3 was constrained to be 1 − occ(Si1), and the occupancy of C2 was constrained to equal the occupancy of Si1. This model of the disorder resulted in percent occupancies of Si in the two sites, Si1 and Si3, of 84% and 16%, respectively.

Crystallographic data for compounds **4a** and **10a** are listed in Table 2, and selected bond lengths and bond angles are given in Table 1 for **4a** and Table 5 for **10a**; full details are given in the Supporting Information.

Acknowledgment. We thank Drs. Frederick Hollander and Patricia Goodson for solving the crystal structures of **4a** and **10a**, the National Institutes of Health (Grant No. GM-25459) for financial support of this work, and Prof. Kristopher McNeill (University of Minnesota) and Dr. Mark Aubart (Ato-Fina) for fruitful discussions. The Center for New Directions in Organic Synthesis is supported by Bristol-Myers Squibb as Sponsoring Member.

Supporting Information Available: Tables of concentrations used in the kinetic runs, one kinetic plot, and crystallographic data for **4a** and **10a**. This material is available free of charge via the Internet at http://pubs.acs.org.

OM010091O

(36) XPREP, version 5.03 (part of the SHELXTL Crystal Structure Determination Package); Siemens Industrial Automation, Inc., 1995.
(37) Sheldrick, G. SADABS: Siemens Area Detector Absorption correction program; Siemens Industrial Automation, Inc., 1996.
(38) teXsan: Crystal Structure Analysis Package; Molecular Structure Corp., 1985 and 1992.